**NASA TECHNICAL MEMORANDUM**

Report No. 53899



# RESULTS OF AN EXPERIMENTAL TURBULENT BOUNDARY LAYER CONTROL INVESTIGATION

By William W. Clever, II
Aero-Astrodynamics Laboratory

September 11, 1969

**NASA**

*George C. Marshall Space Flight Center*
*Marshall Space Flight Center, Alabama*

TECHNICAL REPORT STANDARD TITLE PAGE

| 1. REPORT NO. | 2. GOVERNMENT ACCESSION NO. | 3. RECIPIENT'S CATALOG NO. |
|---|---|---|
| NASA TM X-53899 | | |

| 4. TITLE AND SUBTITLE | 5. REPORT DATE |
|---|---|
| RESULTS OF AN EXPERIMENTAL TURBULENT BOUNDARY LAYER CONTROL INVESTIGATION | September 11, 1969 |
| | 6. PERFORMING ORGANIZATION CODE |
| 7. AUTHOR(S) William W. Clever, II | 8. PERFORMING ORGANIZATION REPORT # |
| 9. PERFORMING ORGANIZATION NAME AND ADDRESS<br>NASA<br>George C. Marshall Space Flight Center<br>Marshall Space Flight Center, Alabama 35812 | 10. WORK UNIT NO. |
| | 11. CONTRACT OR GRANT NO. |
| 12. SPONSORING AGENCY NAME AND ADDRESS | 13. TYPE OF REPORT & PERIOD COVERED<br>Technical Memorandum |
| | 14. SPONSORING AGENCY CODE |

15. SUPPLEMENTARY NOTES

16. ABSTRACT

Results of a wind tunnel test employing wall rougheners as a means of turbulent boundary layer control are presented. This method is demonstrated as being simple, efficient, and capable of yielding predictable results. Boundary layer thickness increases on the order of 100 percent are shown to be possible without undue flow disturbance and velocity profile distortion. The results are compared with the theoretical growth of a turbulent boundary layer over a flat plate.

| 17. KEY WORDS | 18. DISTRIBUTION STATEMENT<br>PUBLIC RELEASE<br><br>E. D. Geissler<br>Director, Aero-Astrodynamics Laboratory |
|---|---|

| 19. SECURITY CLASSIF. (of this report) | 20. SECURITY CLASSIF. (of this page) | 21. NO. OF PAGES | 22. PRICE |
|---|---|---|---|
| UNCLASSIFIED | UNCLASSIFIED | 39 | |

MSFC - Form 3292 (May 1969)

TABLE OF CONTENTS

TECHNICAL MEMORANDUM X-53899

# RESULTS OF AN EXPERIMENTAL TURBULENT BOUNDARY LAYER CONTROL INVESTIGATION


## SUMMARY

The results of a wind tunnel test employing wall rougheners as a means of turbulent boundary layer control are presented. Velocity profiles and surface pressure distributions were measured over a roughened solid side wall model for varying Mach and Reynolds numbers, and the data obtained for various roughener heights are compared with that obtained over a smooth wall.

The test results show Reynolds number effects to be insignificant, boundary layer thickness increases of approximately 100 percent to be possible without undue flow distortion, and boundary layer growth to be the same as that over a smooth plate at a finite distance behind the rougheners. This method gives every indication of being an excellent means of boundary layer control.


## I. INTRODUCTION

A method of boundary layer control that is simple to use and yields predictable results is often desirable in wind tunnel testing. The method of roughening a surface has traditionally been used to produce transition from a laminar to a turbulent boundary layer. It has been suggested, however, that the turbulent boundary layer thickness over a flat plate may be increased by roughening a short section of the plate ahead of the portion over which the increased thickness is desired.* This results in an increase of the skin friction coefficient over the roughened section of the plate, and a corresponding increase of the boundary layer thickness downstream of the rougheners. Thus, the purpose of this test was to investigate the boundary layer characteristics behind a roughened section of a flat plate and to determine whether or not this method of boundary layer control is suitable for wind tunnel testing.

---

*Unpublished note, McDonnell Douglas Corporation.

As a simple method of roughening the plate, it was originally planned to use small "short angle" sections fastened to the surface. This technique would have made it possible to empirically predict the proper spacing and height into the airstream for the "short angles" by using experimental data reported by Schlichting [1]. This method was discarded, however, in favor of using roll pins as the roughener elements which allowed the height into the airstream to be varied at will, even though no experimental data were available for this type of roughener.

Because this method was later used in a panel flutter test, it was necessary to establish the validity of this type of boundary layer control.

## II. EMPIRICAL METHOD

Reference 1 contains results of experiments conducted by J. Nikuradse [2,3,4] on both flat plates and roughened pipes. The results of his studies showed that the velocity profiles were similar if nondimensional velocities were plotted against $y/\delta^*$, where $\delta^*$ is the displacement thickness. The skin friction coefficients and the momentum thicknesses were calculated based on these measured profiles and the following equations were obtained:*

$$u/U_\infty = 0.737(y/\delta^*)^{0.1315} \tag{1}$$

$$\delta^*/\theta = 1.3. \tag{2}$$

(This analysis is primarily based upon reference 1 and liberal use is made of this reference here.) Also, from the momentum equation with zero pressure gradient, we obtain

$$C_F = 2\theta(\ell)/\ell, \tag{3}$$

where

u is the velocity in the layer at point y,

$U_\infty$ is the boundary layer edge velocity,

*See footnote on page 1.

$\delta^*$ is the displacement thickness,

$\theta$ is the momentum thickness,

$C_F$ is the total skin friction coefficient,

$\ell$ is the length of the plate.

Combining equations (1), (2), and (3) and using the relationship that y equals $\delta$ and $u/U_\infty$ equals 1 at the edge of the boundary layer, the following relation is obtained:

$$\delta(\ell) = 6.619\ C_F \ell, \tag{4}$$

where $\delta$ is the boundary layer thickness.

Figure 21.11 of reference 1 shows the skin friction coefficient as a function of the ratio of plate length to sand grain size and the plate Reynolds number. For the completely rough flow regime, the skin friction is given by

$$C_F = (1.89 + 1.60\ \log_{10}(\ell/ks))^{-2.5} \tag{5}$$

for $10^2 \leq \ell/ks \leq 10^6$. In equation (5) the skin friction coefficient is a function only of plate length and sand grain size; whereas, for the smooth plate, the skin friction coefficient is a function of the Reynolds number.

Schlichting [1] determined experimentally the boundary layer depths on plates using spheres, hemispheres, cones, and "short angles" as the roughening devices. From these experiments, he determined the equivalent sand grain size (ks). Figure 20.24 of reference 1 summarizes the results of his experiment.

By using the equivalent sand grain size of a given distribution of roughness elements, it is possible to predict the boundary layer thickness as follows:

(1) Obtain ks from Figure 20.24 (Ref. 1).

(2) Use this ks in equation (5).

(3) Use the resulting $C_F$ in equation (4) to obtain $\delta(\ell)$.

This procedure yields the boundary layer depth as a function of length over the roughened portion of the plate only.

Since only a short section of the plate is to be roughened, the combined effects of boundary layer growth over both smooth and roughened portions of the plate must be considered. This can be done by plotting $\delta(\ell)$, obtained in step 3 above, versus distance along the roughened plate. The boundary layer thickness thus obtained for a specific length of roughened plate may be used to obtain an equivalent length of smooth plate from a plot of the boundary layer thickness versus distance along a smooth plate.

Thus, a new length can be defined as

$$\ell a \equiv \ell_E - \ell_R,$$

where $\ell_R$ is the length of the roughened section, and $\ell_E$ is the equivalent smooth plate length. The boundary layer thickness at the end of a plate, of length $\ell$, having a roughened section of length $\ell_R$, may then be calculated as the thickness at the end of a smooth plate of length $\ell + \ell a$.

Using this method and a roughener distribution, given in Figure 20.24 of reference 1, yielding an equivalent sand grain size (ks) of 0.567 inches for "short angles," a 42 percent increase in the boundary layer thickness was predicted for a roughened section eight inches long.

An equivalent sand grain size was not available for the roll pins, however. Thus, the same distribution of roughness elements was used for the roll pins as would have been used for the "short angles."

## III. TEST MODEL

The model used for this experiment was an existing solid side wall that had been previously fabricated for the transonic test section of the MSFC 14 x 14-inch trisonic wind tunnel. The first 7.5 inches of this plate were roughened by placing 0.315-inch-diameter roll pins through the plate in an arrangement as shown in Figures 1 and 2. It was possible to vary the height of the pin protrusion into the airstream from a smooth plate case to at least 0.5 inches.

The roll pins used in this test were commercially available 0.315-inch-diameter hollow steel tubes one inch long and split down one side.

The purpose of the split side is to provide a spring-tension, friction fit when placed through a hole 0.315 inch in diameter. Thus, it was not necessary to weld or solder the pins in place, and it was a simple matter to adjust their height of protrusion.

## IV. INSTRUMENTATION

The data collected during this test included six static wall pressure measurements, and twelve total pressure measurements on a boundary layer rake. The locations of the static pressure ports and the locations of the probe tips of the boundary layer rake for the three rake positions used are indicated in Figure 2. The boundary layer rake probe height distribution is shown in Table 1.

Table 1. Boundary Layer Rake Tube Height Distribution

| Tube Number | Height Above Plate (inches) |
|---|---|
| 1 | 0.060 |
| 2 | 0.130 |
| 3 | 0.200 |
| 4 | 0.270 |
| 5 | 0.340 |
| 6 | 0.410 |
| 7 | 0.480 |
| 8 | 0.550 |
| 9 | 0.700 |
| 10 | 1.095 |
| 11 | 1.575 |
| 12 | 2.075 |

These pressures were measured with the wind tunnel scani-valve system which employed 12.5 PSID transducers calibrated at five counts per millimeter of mercury.

## V. TEST PROCEDURE

Three model configurations tested were designated as follows:

Configuration (1): Flat plate, roll pins down level with the plate and the holes filled with wax.

Configuration (2): Roll pins protruding 0.118 inch above the plate and into the airstream.

Configuration (3): Roll pins protruding 0.250 inch above the plate and into the airstream.

Each configuration was tested at three different Mach numbers ($M_\infty$ = 1.2, 1.3, and 1.46) with three different boundary layer rake positions for each Mach number. Also, the effects of Reynolds number were investigated during the early part of the test by running each Mach number at two different total pressures. These corresponded to $R_\ell = 7 \times 10^6$ per foot for a total pressure of 7 psig and $R_\ell = 9 \times 10^6$ per foot for a total pressure of 15 psig.

The following wind tunnel parameters were also recorded for each run:

(1) Total pressure,

(2) Mach number,

(3) Test section static pressure,

(4) Stagnation temperature.

## VI. DATA REDUCTION

The raw data from this test were punched out on computer cards by means of an "on-line" system, and were then used with a computer program that converted from counts per millimeter of mercury gauge pressure to absolute pressure in pounds per square inch. The following equations were also included in the program:

$$\frac{P_{T_2}}{P_{T_1}} = \left[\frac{6M_L^2}{M_L^2 + 5}\right]^{7/2} \left[\frac{6}{6M_L^2 - 1}\right]^{5/2} \qquad (M_L > 1 \text{ only}) \qquad (6)$$

$$\frac{P_{T_2}}{P_n} = \left[\frac{6M_L^2}{5}\right]^{7/2} \left[\frac{6}{7M_L^2 - 1}\right]^{5/2} \qquad \text{(Rayleigh Pitot Formula)} \quad (M_L > 1 \text{ only}) \qquad (7)$$

$$\frac{P_{T_1}}{P_n} = \left[1 + \frac{M_L^2}{5}\right]^{7/2} \qquad (M_L < 1) \text{ (no shock)} \qquad (8)$$

$$\frac{U_L}{U_\infty} = \frac{M_L}{M_\infty} \left[\frac{1 + \frac{\gamma-1}{2} M_\infty^2}{1 + \frac{\gamma-1}{2} (M_L/M_\infty)^2 M_\infty^2}\right]^{1/2} \qquad (9)$$

where $P_{T_1}$ and $P_{T_2}$ are the total pressures indicated in Figure 3, $P_n$ is the static pressure as indicated, and $M_L$ is the Mach number directly ahead of the pressure tube but also ahead of the bow shock which may or may not exist ahead of the pressure tube. $U_L$ and $U_\infty$ are the local velocities ahead of the pressure tube and the velocity of the free stream, respectively.

These equations were used as follows:

Step (1): If $P_n/P_{T_2} \leqq 0.5283 \equiv M_L > 1$, use equation (7) and solve for $M_L$ for each probe, and use equation (6) and solve for $P_{T_1}$.

Step (2): If $P_n/P_{T_2} > 0.5283 \equiv M_L < 1$, use equation (8) and solve for $M_L$ for each probe (note that in this case $P_{T_1} \equiv P_{T_2}$.

Step (3): Compute $(M_L/M_\infty)$ for each probe, and use equation (9) to solve for the velocity ratio $(U_L/U_\infty)$ for each probe.

## VII. TEST RESULTS

Velocity ratio profiles showing the effect of two different Reynolds numbers are presented in Figures 4a through 4i. The Mach number and boundary layer rake positions are shown on each figure. The two Reynolds numbers ($7 \times 10^6$ and $9 \times 10^6$ per foot) were achieved by running two different total pressures (7 psig and 15 psig, respectively) for each Mach number. This comparison was made for configuration 2 only (roll pins protruding 0.118 inch). These figures show that the effect of changing Reynolds number was insignificant.

The effects of two different pin heights as compared with smooth plate flow are shown in Figures 5a through 5i. The Mach number, boundary layer rake position, and the pin height, along with the approximate boundary layer thickness and the percentage of increase in the boundary layer thickness over the flat plate value, are indicated on each figure. The boundary layer thickness was taken to be the distance from the plate where the velocity ratio achieved 98 percent of its free stream value. A definite increase in the boundary layer thickness is apparent; however, the boundary layer profile tends to "flatten." This flattening may be regarded as a departure from the type of profile expected for a smooth plate. For configuration 2 (pin height = 0.118 inch), this situation improves as the Mach number and the distance from the roughening elements are increased. For configuration 3 (pin height = 0.25 inch), however, the velocity profile shows definite distortion even at the aft boundary layer rake position and at the highest Mach number tested.

Pressure coefficient variations over the length of the plate are shown in Figures 6a through 6c. Here the pressure coefficient is defined as

$$C_p \equiv (p_n - p_\infty)/q_\infty$$

where

$p_\infty$ = tunnel static pressure,

$p_n$ = measured static pressure at different points on the plate,

$q_\infty$ = free stream dynamic pressure.

All test conditions are indicated on each figure. The pressure coefficient is plotted versus the normalized distance along the plate (X/L, where L is the length of the plate: 40 inches). The main point of interest here is the amount of deviation from a pressure coefficient of zero which would correspond to undisturbed flow. Since it is generally accepted that deviations of the pressure coefficient between the values of $-0.1 \leqq C_p \leqq + 0.1$ are insignificant, the flow may be regarded as undisturbed. The value of the pressure coefficient was well within these limits for all cases tested. A rather curious result here is an improvement in the flow in some cases, when the rougheners are used. This would seem to indicate a slight amount of rough flow from the wind tunnel itself.

The growth of the boundary layer along the plate for all conditions tested is shown in Figure 7. There is a tendency (except for two cases, M = 1.3 with pins up 0.118 inch and M = 1.46 with pins up 0.250 inch)

in the slope or rate of boundary layer growth to decrease between the second and third rake positions. In Figure 8 these growth rates are compared to the theoretical growth of a turbulent boundary layer over a smooth plate. Since it was expected that the growth rate of the boundary layer would return to that over a smooth plate, with a shift in distance along the plate, of course, the value of the boundary layer thickness at the second rake position was placed on the theoretical curve of Figure 8. This makes it possible to compare the slope of the boundary layer growth, both in front of and behind the second rake position, with the slope of the theoretical curve. Excellent agreement between the theoretical and experimental values can be seen from this figure. The smooth plate values fall right along the theoretical curve as they should, and the slope between the second and third rake positions is almost identical to that of the theoretical boundary layer growth when the roughenerers were used, with the previously mentioned exceptions.

## VIII. CONCLUSIONS AND RECOMMENDATIONS

The following conclusions can be made from the foregoing results of this test:

(1) Reynolds number effects show no significant changes in either the boundary layer thickness or velocity profile shape over the roughened plate. This is in agreement with reference 1 for the completely rough flow regime.

(2) This method of boundary layer control can yield a tremendous increase in the thickness of the layer (over 100 percent). However, it should be remembered that the higher the roughenerers protrude into the airstream, the more the velocity profile is "flattened" or deviates from a smooth plate type profile.

(3) No significant flow disturbance is indicated from the pressure coefficient data; in fact, excellent flow is indicated for all configurations.

(4) At a finite distance behind the roughenerers, the rate of growth of the boundary layer returns to that of a turbulent boundary layer over a smooth plate.

This method gives every indication of being an excellent means of boundary layer control. It is simple to use and yields predictable results as long as the roughener distribution, the height, and the distance behind the roughenerers are judiciously chosen.

For this particular type, size, and distribution of rougheners, it is recommended that the height of roughener protrusion into the airstream not exceed 0.118 inch, because excessive distortion of the velocity profile may result. It is further recommended that at least 19 inches of smooth plate be allowed behind the rougheners for the boundary layer to return to its smooth-plate characteristics.

## REFERENCES


1. Schlichting, H., Boundary Layer Theory, 4th ed., McGraw Hill Book Company.

2. Nikuradse, J., "Untersuchungen uber die Geschwindigkeitsverteilung in turbulenten Stromuugen." Thesis Gottingen 1926. VDI-Forschungsheft 281, Berlin (1926).

3. Nikuradse, J., "Gesetzmassigkeit des Turbulenten Stromung in glatten Rohren." Forschungsheft 356 (1932).

4. Nikuradse, J., "Stromungsgesetze in rauhen Rohren." Forschungsheft 361 (1933).

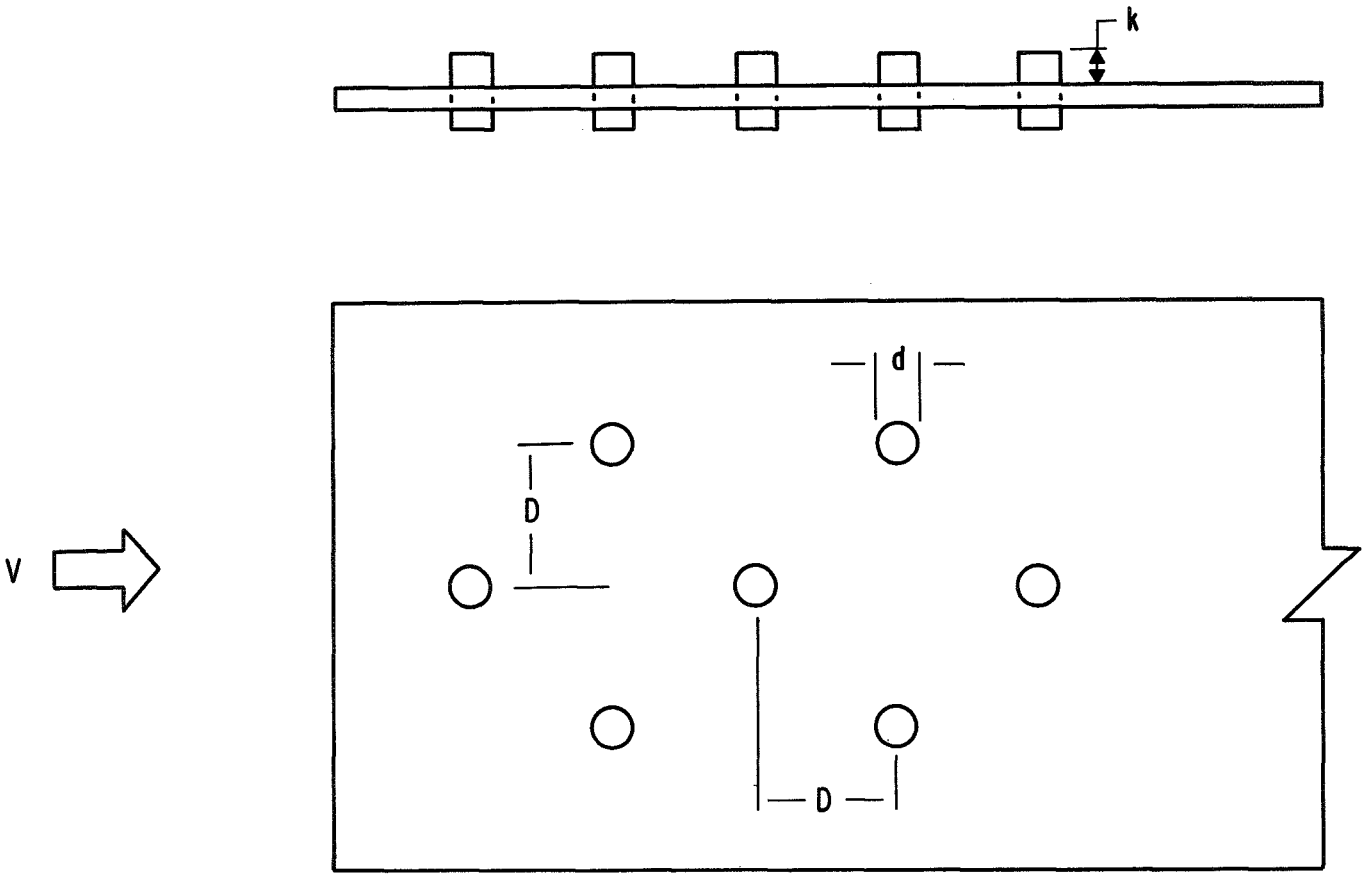


| | k (in) | d (in) | D (in) |
|---|---|---|---|
| CONF. 1 | 0 | 0.315 | 0.8 |
| CONF. 2 | 0.118 | 0.315 | 0.8 |
| CONF. 3 | 0.250 | 0.315 | 0.8 |

FIGURE 1. ROUGHENER GEOMETRY

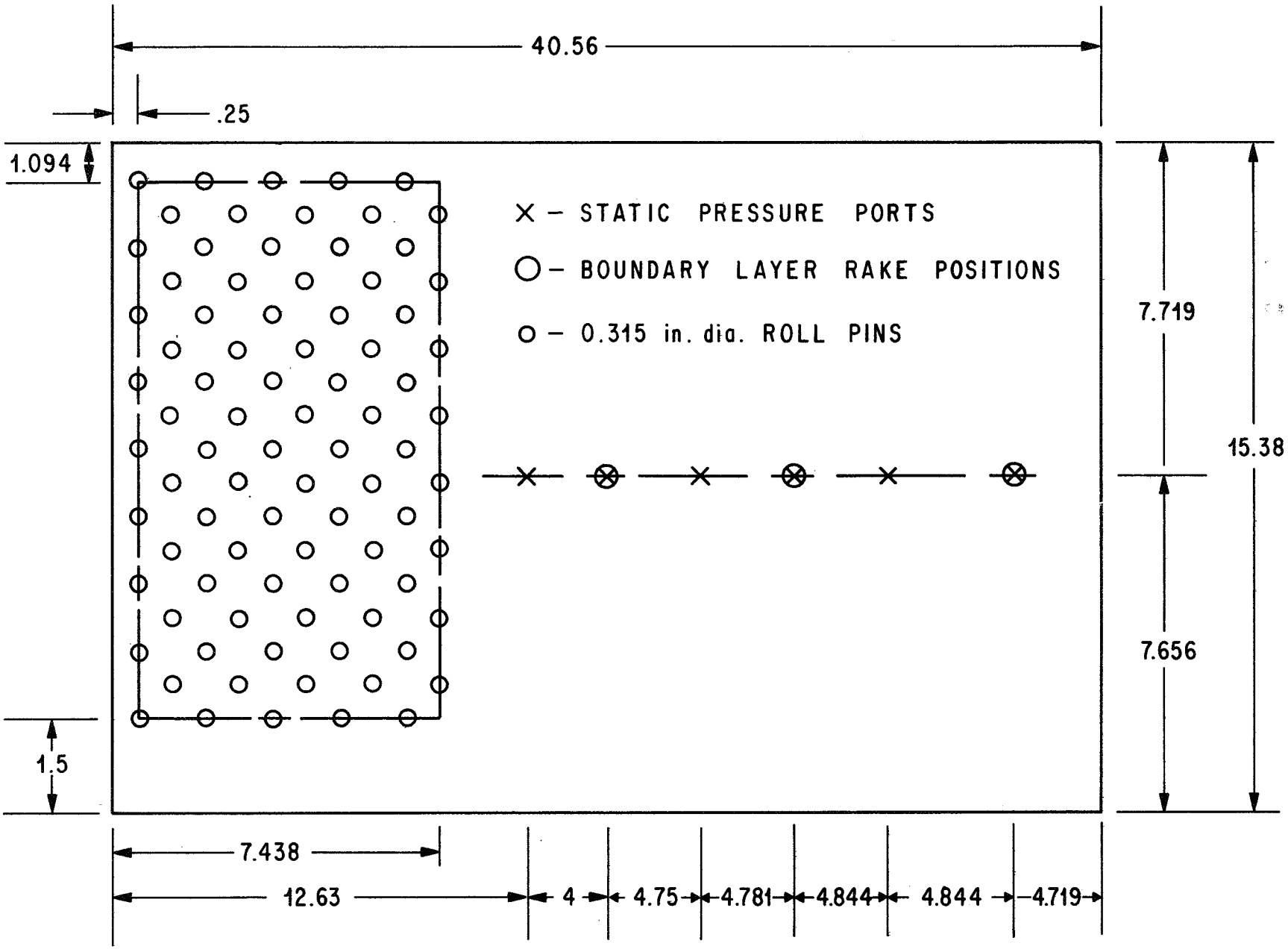


FIGURE 2. MODEL GEOMETRY

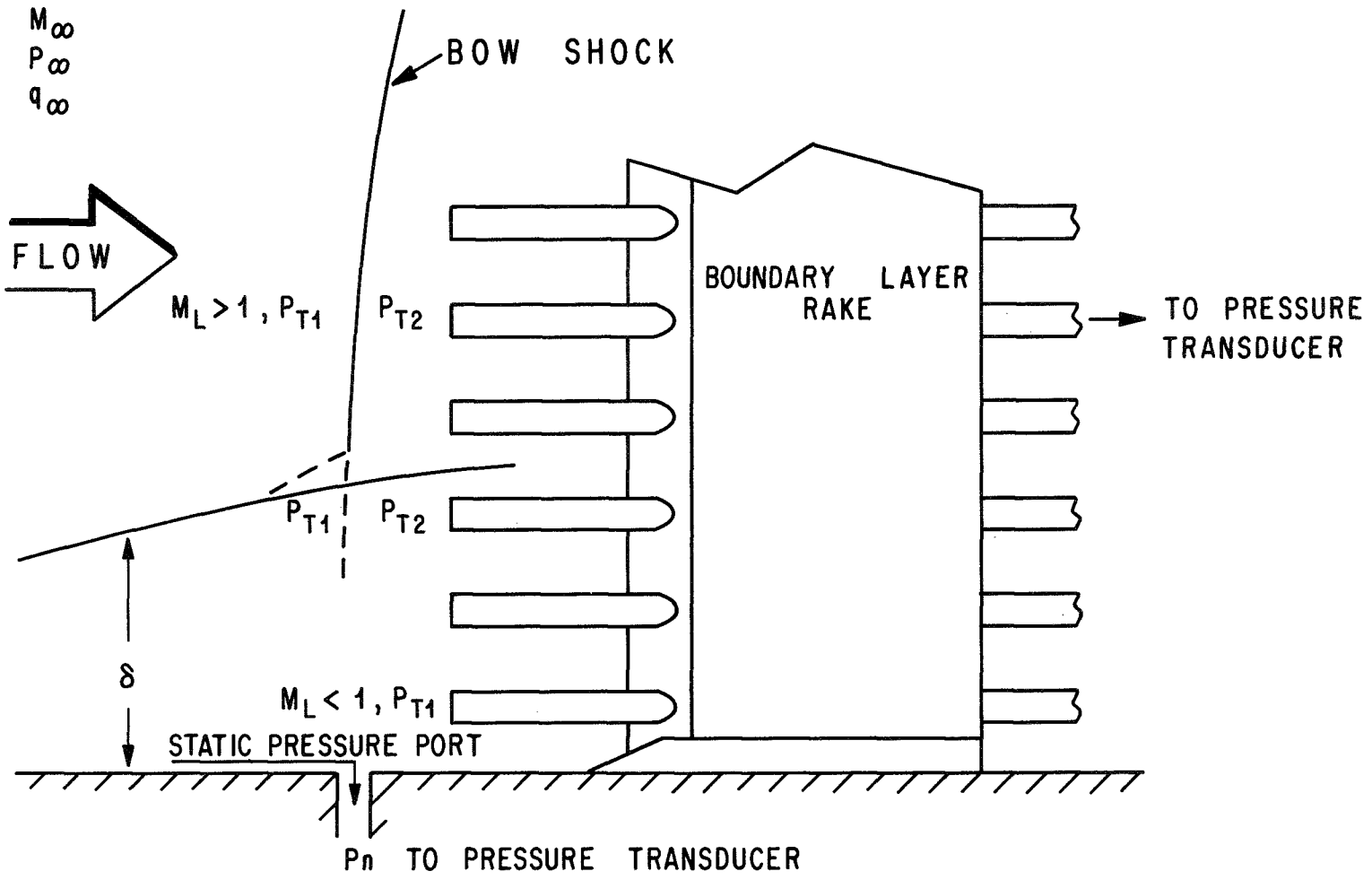


FIGURE 3. LOCATION OF VARIABLES

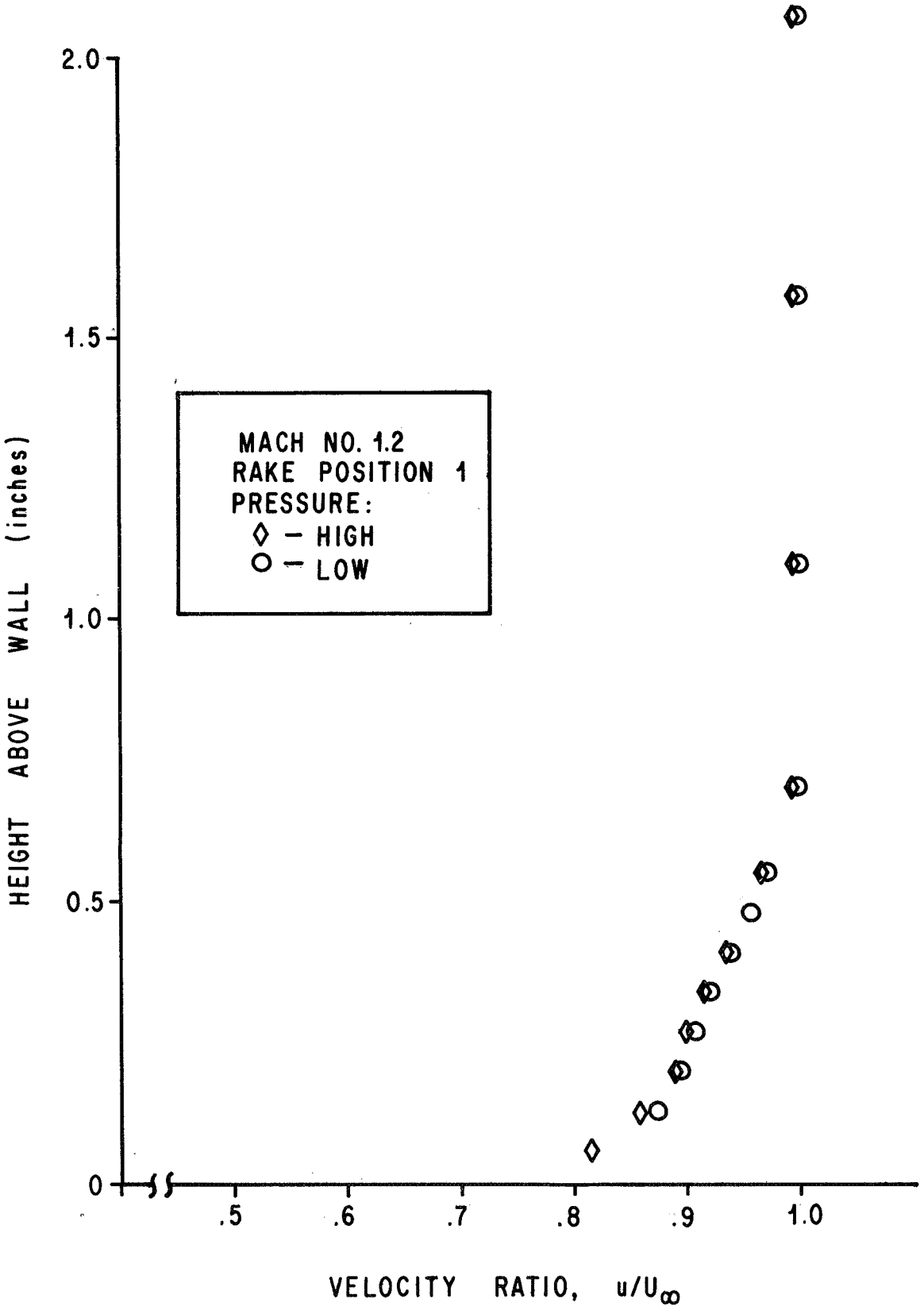


FIGURE 4a. EFFECT OF REYNOLD'S NUMBER ON VELOCITY PROFILE

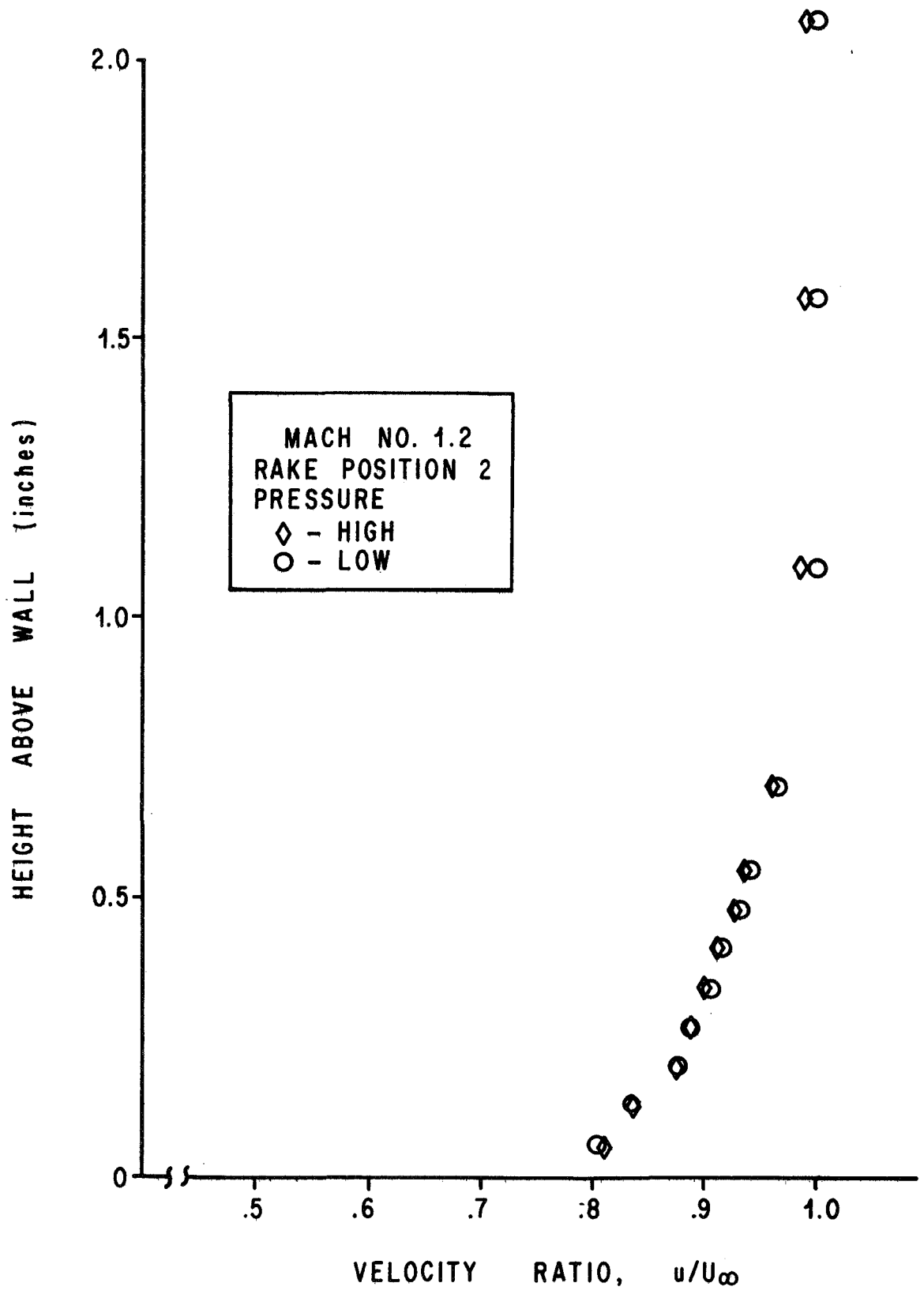
2.0
1.5
1.0
0.5
0
MACH NO. 1.2
RAKE POSITION 2
PRESSURE
◊ - HIGH
O - LOW
HEIGHT ABOVE WALL (inches)
.5
.6
.7
:8
.9
1.0
VELOCITY RATIO, u/U∞

FIGURE 4b

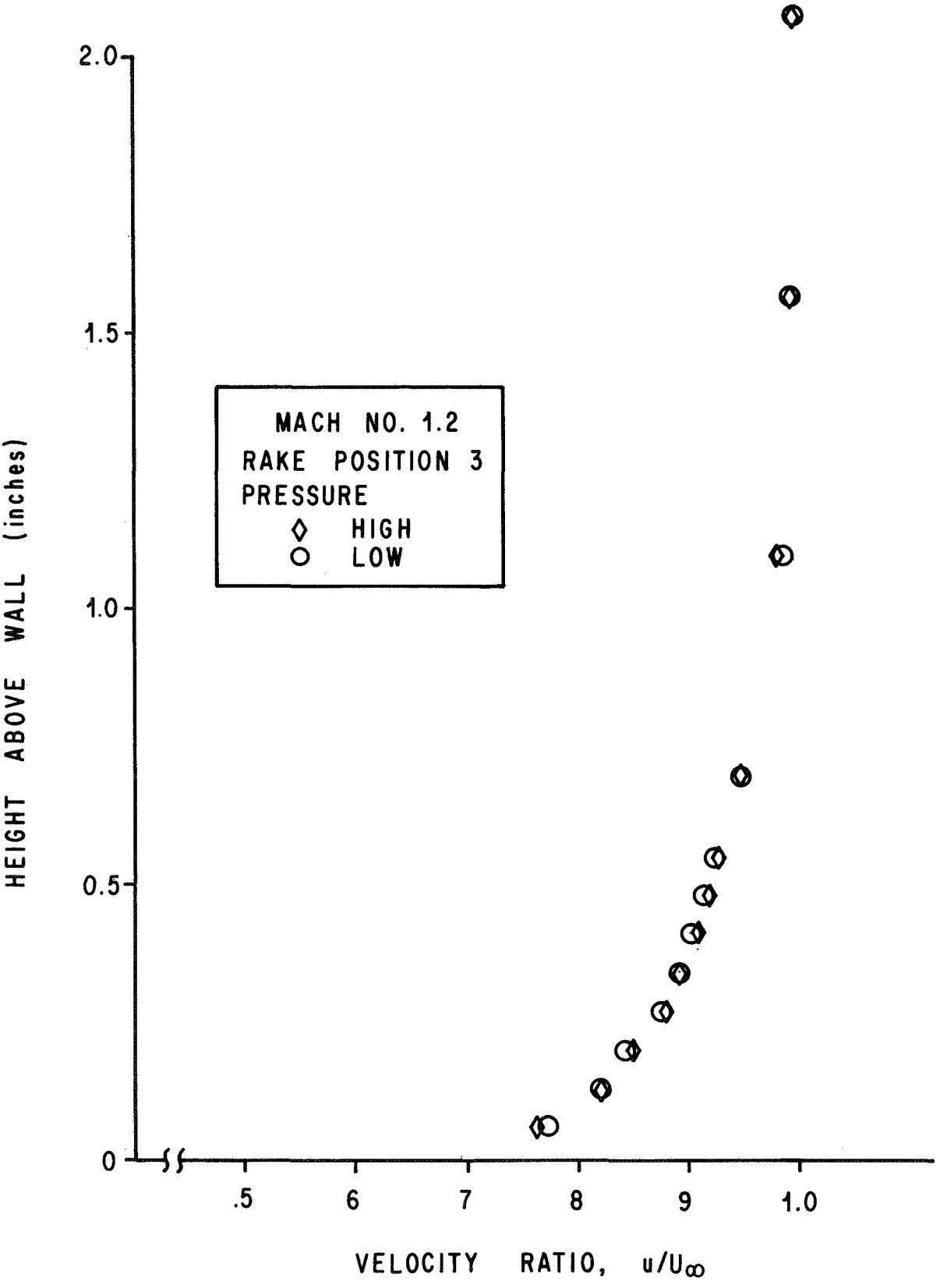
2.0
1.5
1.0
0.5
0
HEIGHT ABOVE WALL (inches)
MACH NO. 1.2
RAKE POSITION 3
PRESSURE
◊ HIGH
○ LOW
.5
6
7
8
9
1.0
VELOCITY RATIO, u/U∞

FIGURE 4c

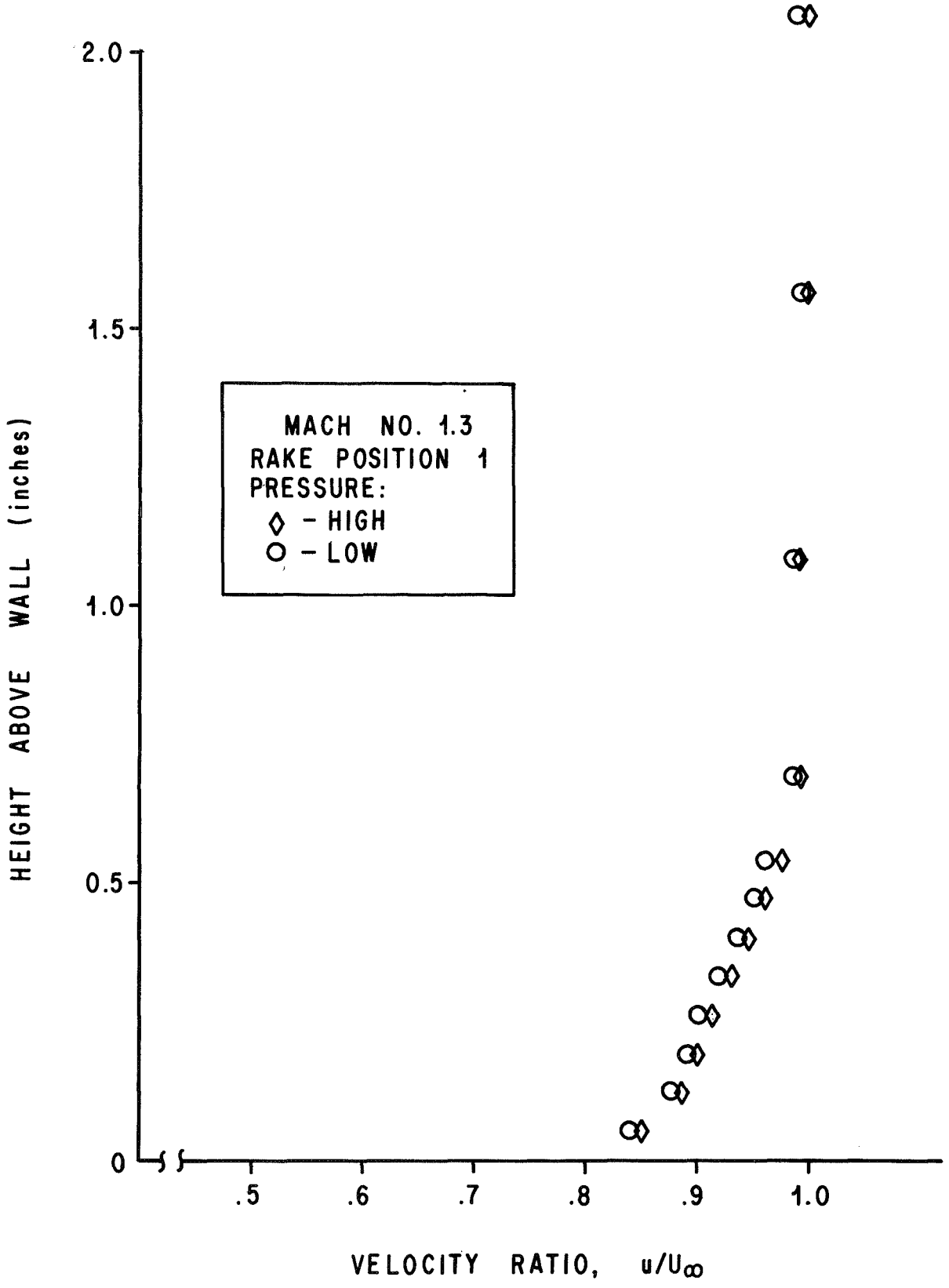
2.0
1.5
1.0
0.5
0
HEIGHT ABOVE WALL (inches)
MACH NO. 1.3
RAKE POSITION 1
PRESSURE:
◊ - HIGH
O - LOW
.5
.6
.7
.8
.9
1.0
VELOCITY RATIO, u/U∞

FIGURE 4d

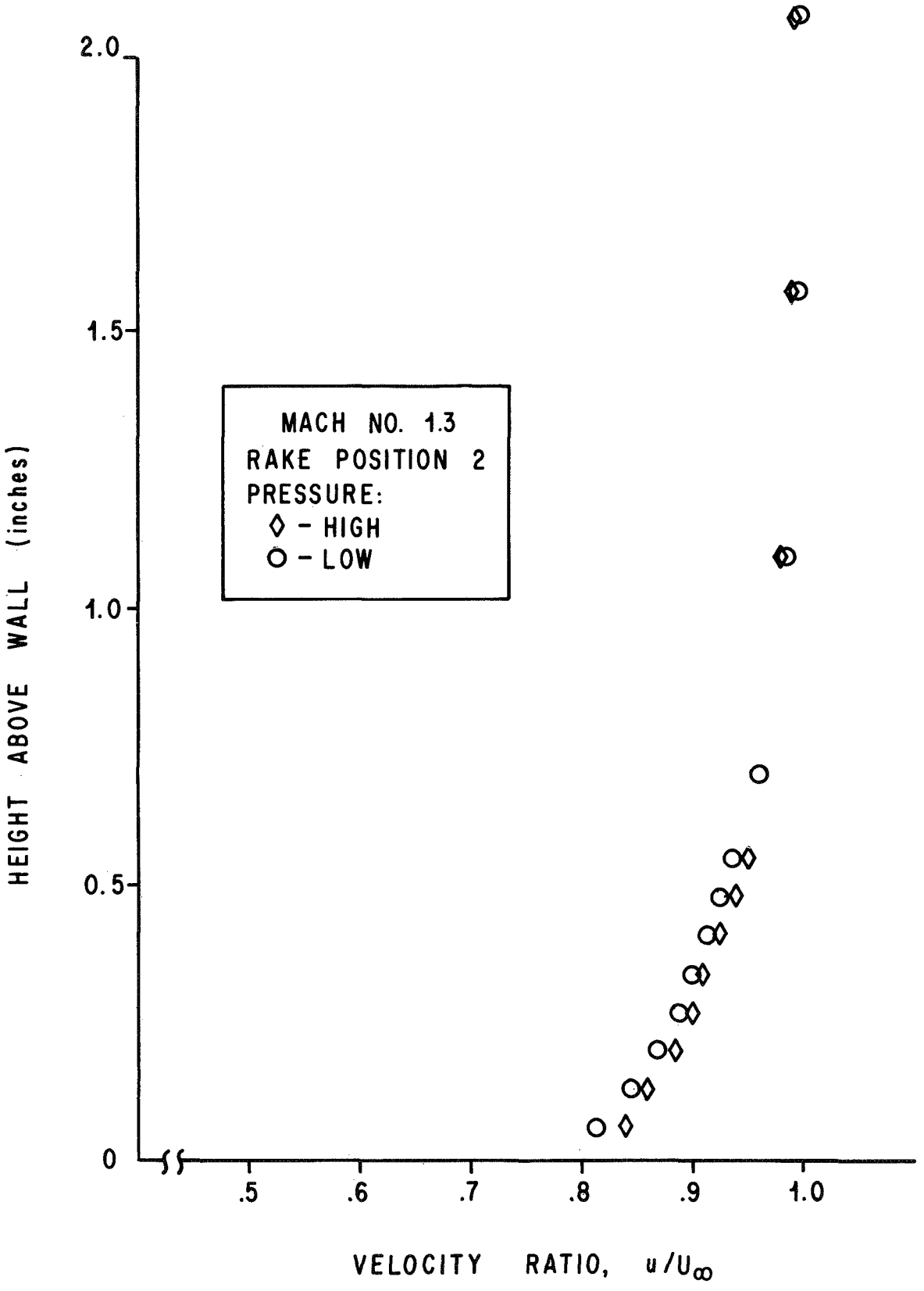
2.0
1.5
1.0
0.5
0
HEIGHT ABOVE WALL (inches)
MACH NO. 1.3
RAKE POSITION 2
PRESSURE:
◊ - HIGH
O - LOW
.5
.6
.7
.8
.9
1.0
VELOCITY RATIO, $u/U_\infty$

FIGURE 4e

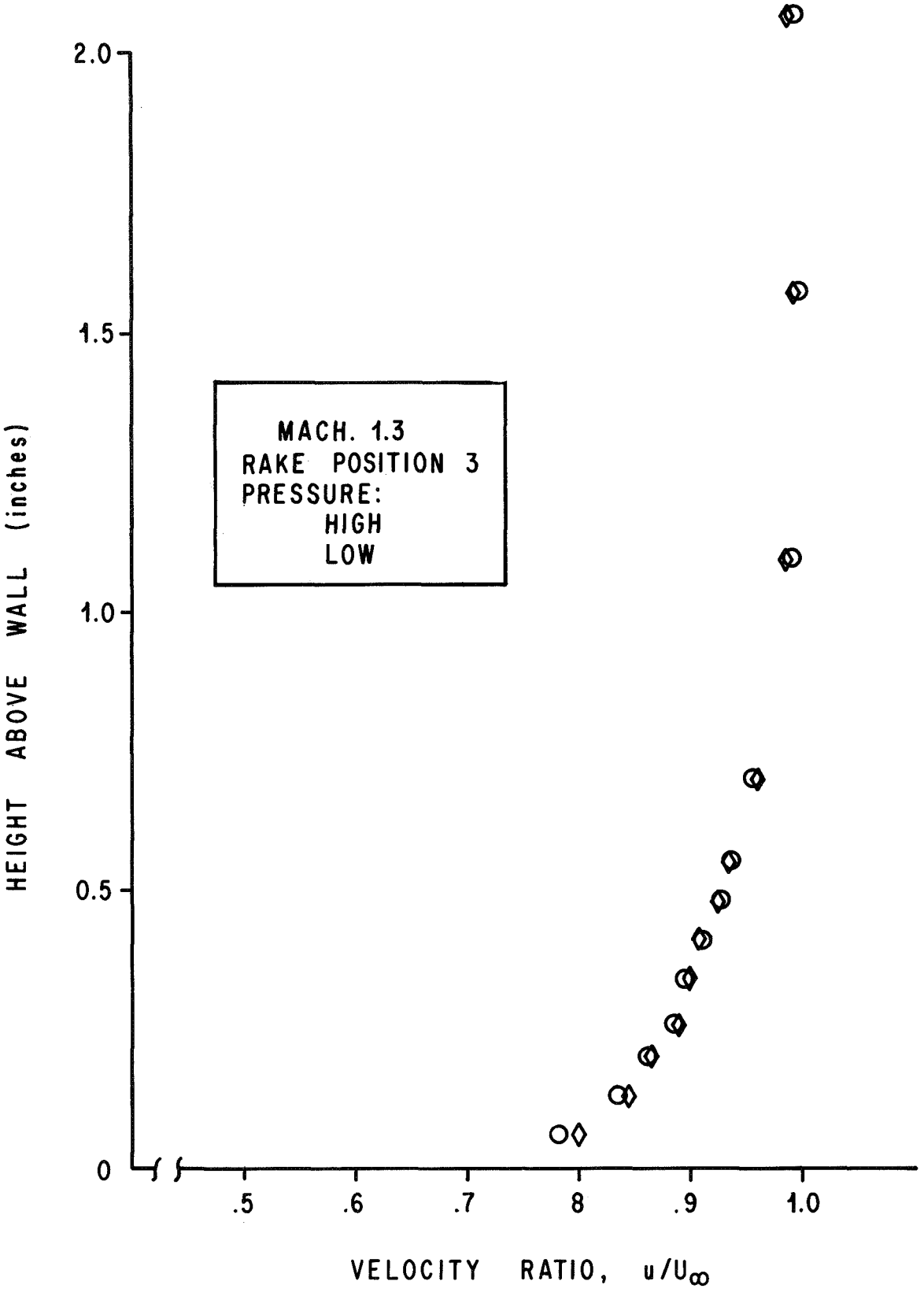
2.0
1.5
1.0
0.5
0
HEIGHT ABOVE WALL (inches)
MACH. 1.3
RAKE POSITION 3
PRESSURE:
HIGH
LOW
.5
.6
.7
.8
.9
1.0
VELOCITY RATIO, u/U∞

FIGURE 4f

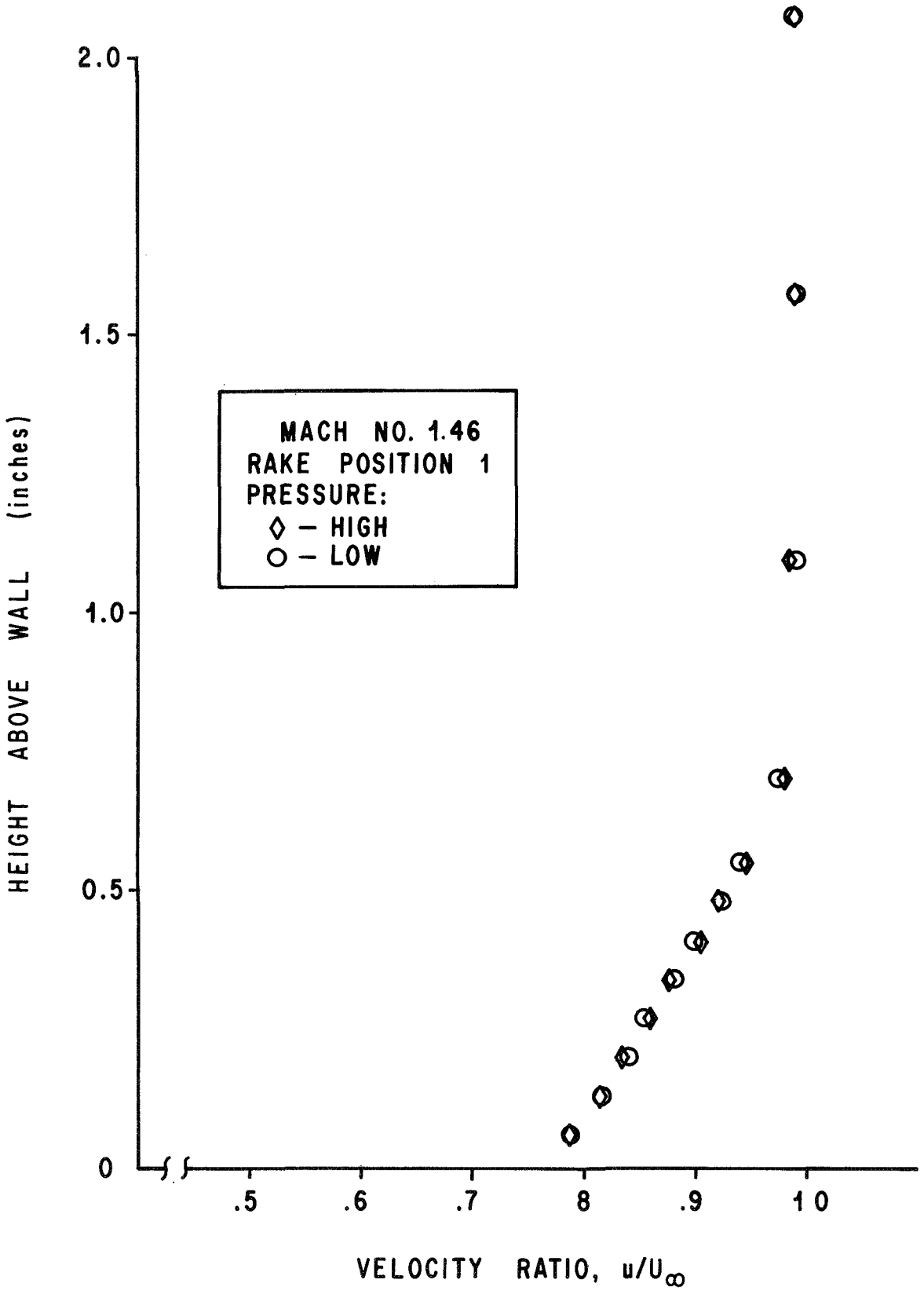
2.0
1.5
1.0
0.5
0
HEIGHT ABOVE WALL (inches)
MACH NO. 1.46
RAKE POSITION 1
PRESSURE:
◊ – HIGH
○ – LOW
.5
.6
.7
8
.9
1 0
VELOCITY RATIO, u/U∞

FIGURE 4g

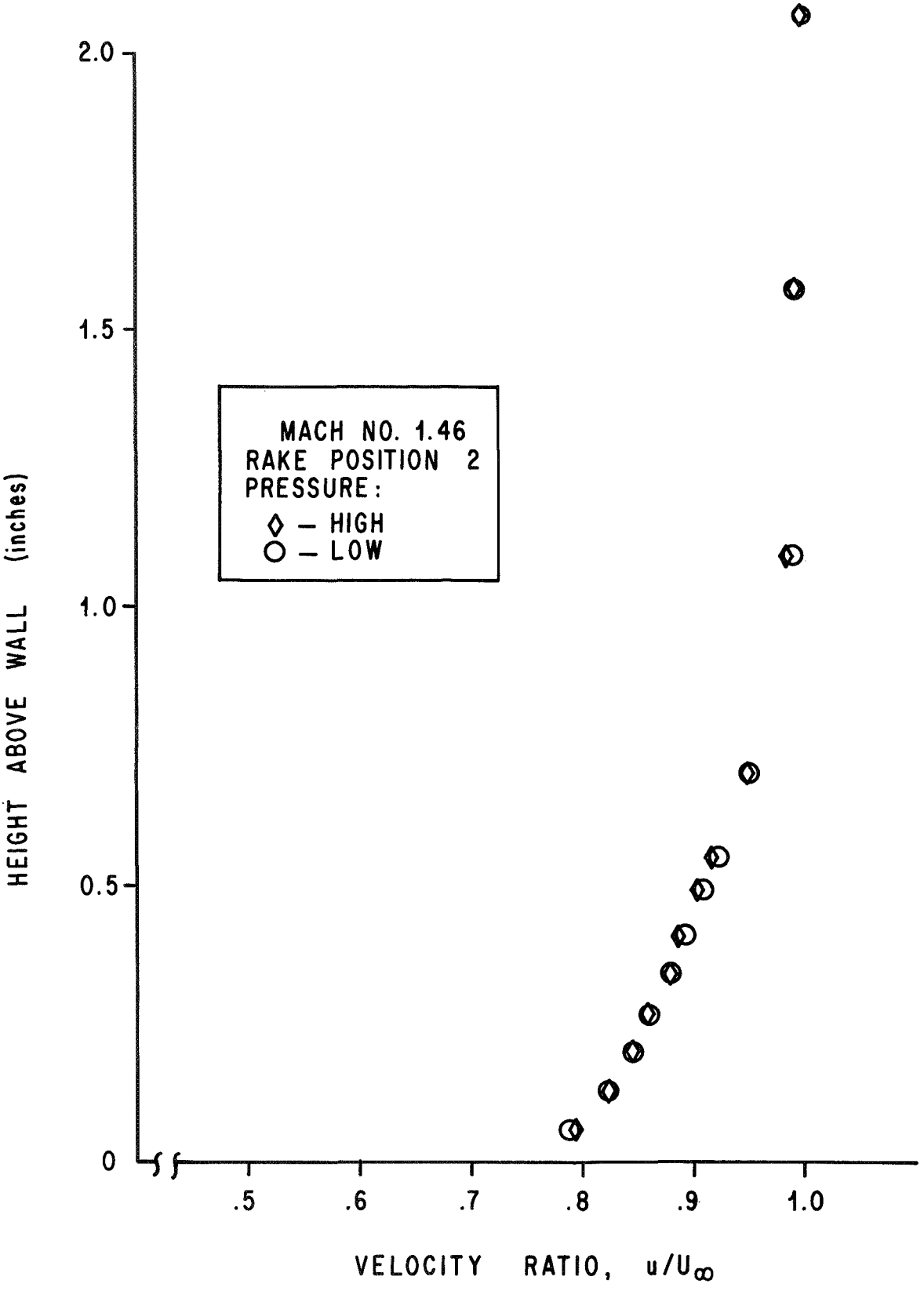
2.0
1.5
1.0
0.5
0
HEIGHT ABOVE WALL (inches)
MACH NO. 1.46
RAKE POSITION 2
PRESSURE:
◊ – HIGH
○ – LOW
.5
.6
.7
.8
.9
1.0
VELOCITY RATIO, u/U∞

FIGURE 4h

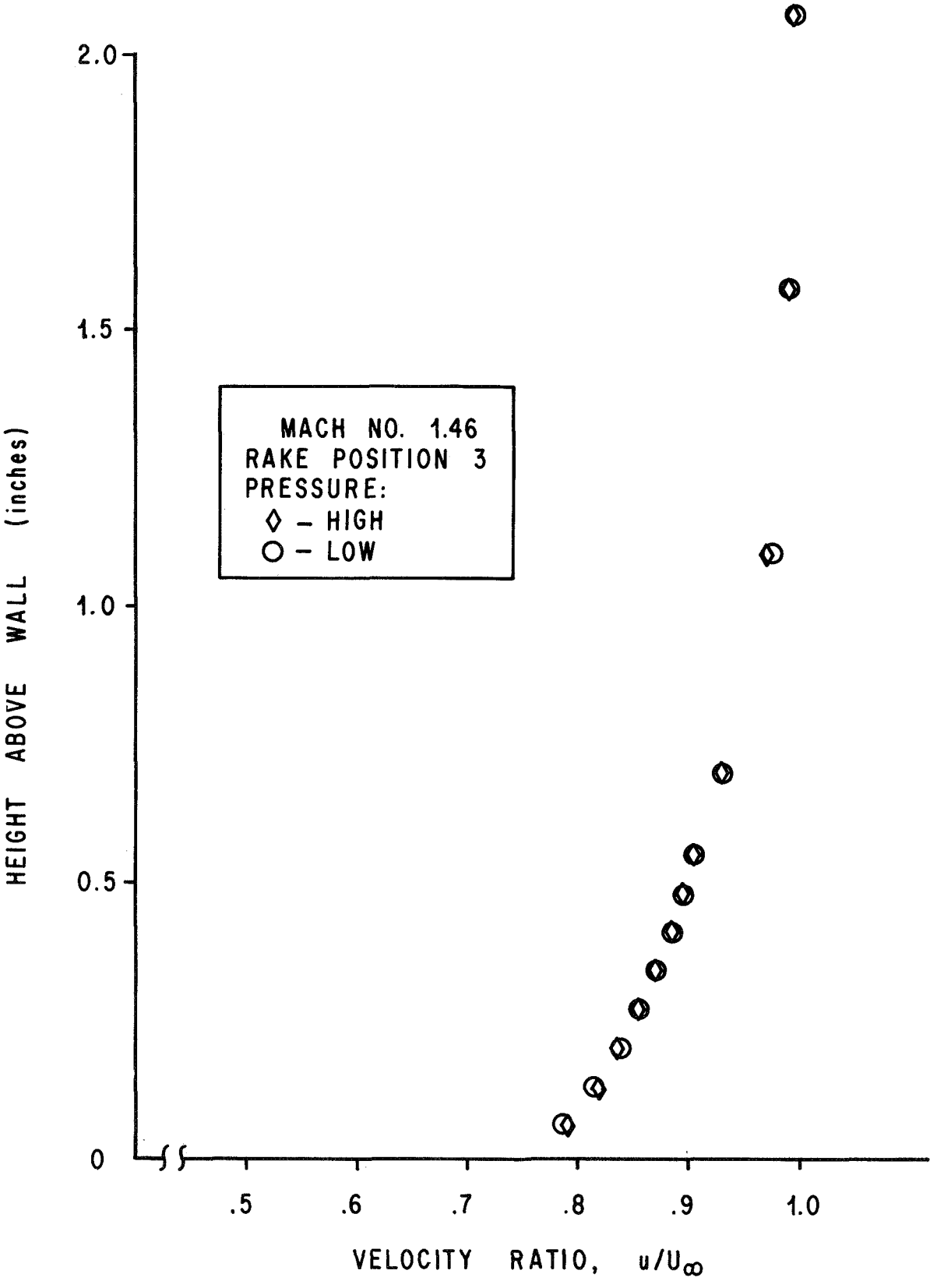
2.0
1.5
1.0
0.5
0
HEIGHT ABOVE WALL (inches)
MACH NO. 1.46
RAKE POSITION 3
PRESSURE:
◊ – HIGH
○ – LOW
.5
.6
.7
.8
.9
1.0
VELOCITY RATIO, u/U∞

FIGURE 4i

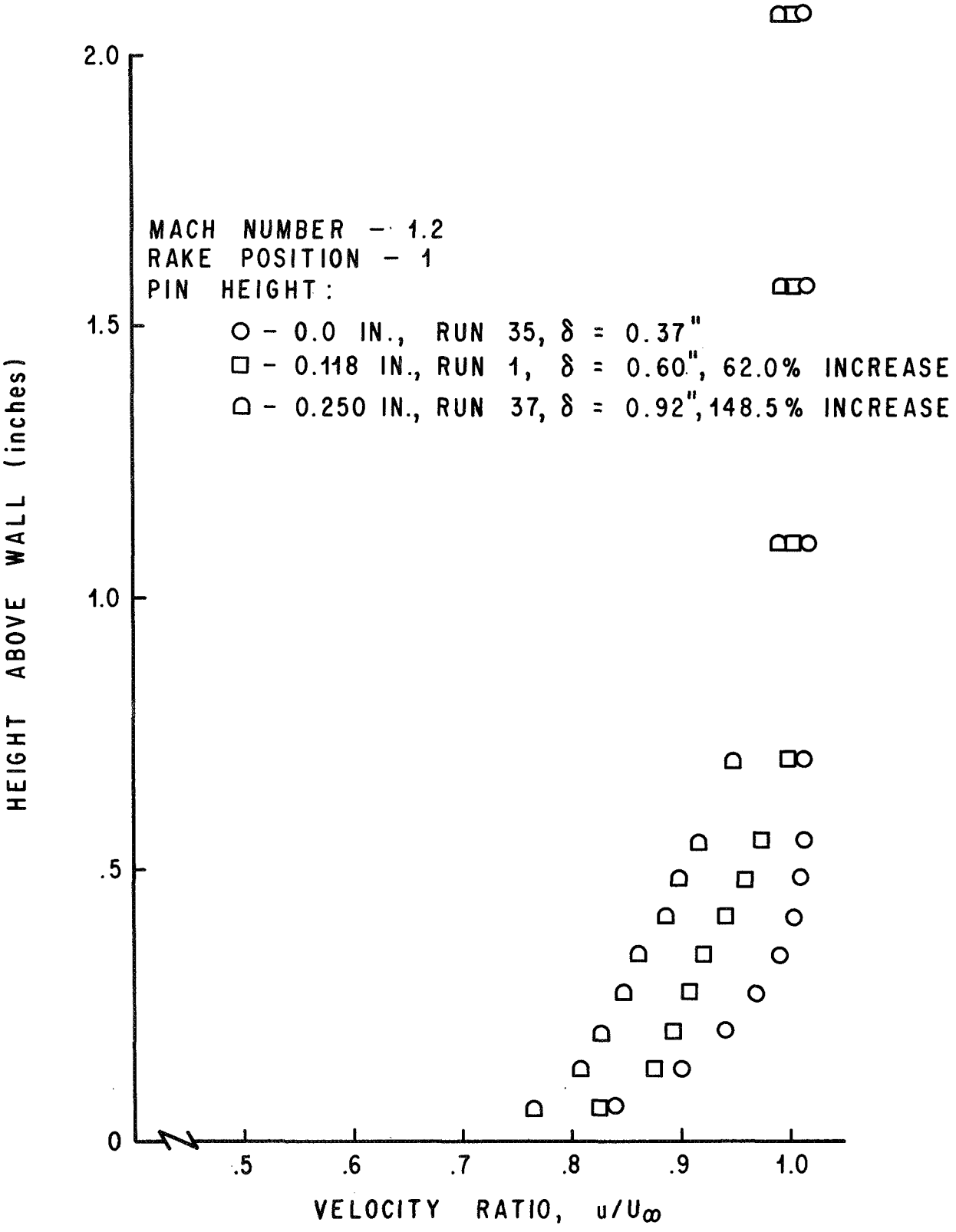


FIGURE 5a. VELOCITY PROFILES

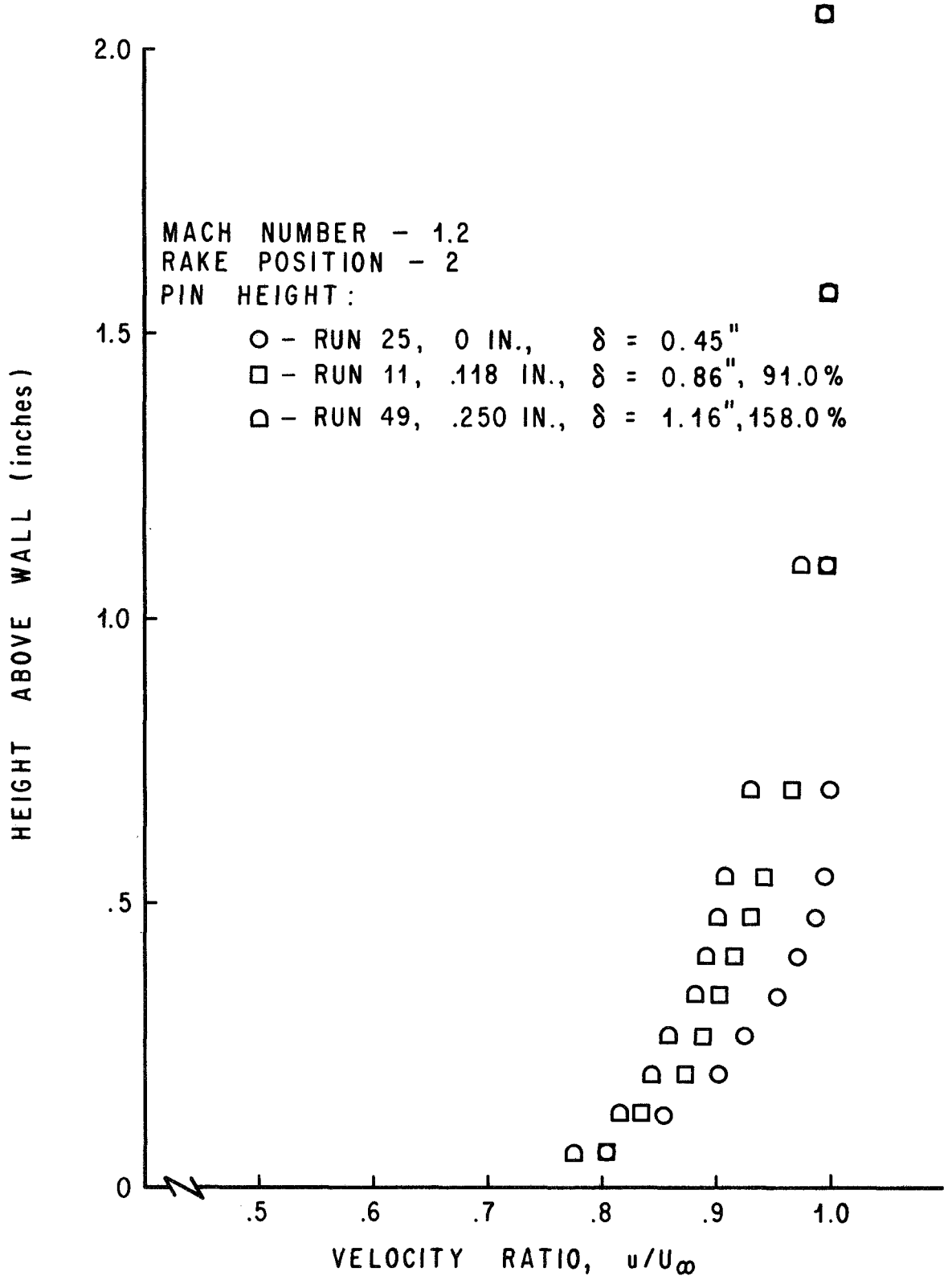
MACH NUMBER – 1.2
RAKE POSITION – 2
PIN HEIGHT:
○ – RUN 25, 0 IN., δ = 0.45"
□ – RUN 11, .118 IN., δ = 0.86", 91.0%
⌂ – RUN 49, .250 IN., δ = 1.16", 158.0%
HEIGHT ABOVE WALL (inches)
2.0
1.5
1.0
.5
0
.5
.6
.7
.8
.9
1.0
VELOCITY RATIO, u/U∞

FIGURE 5b

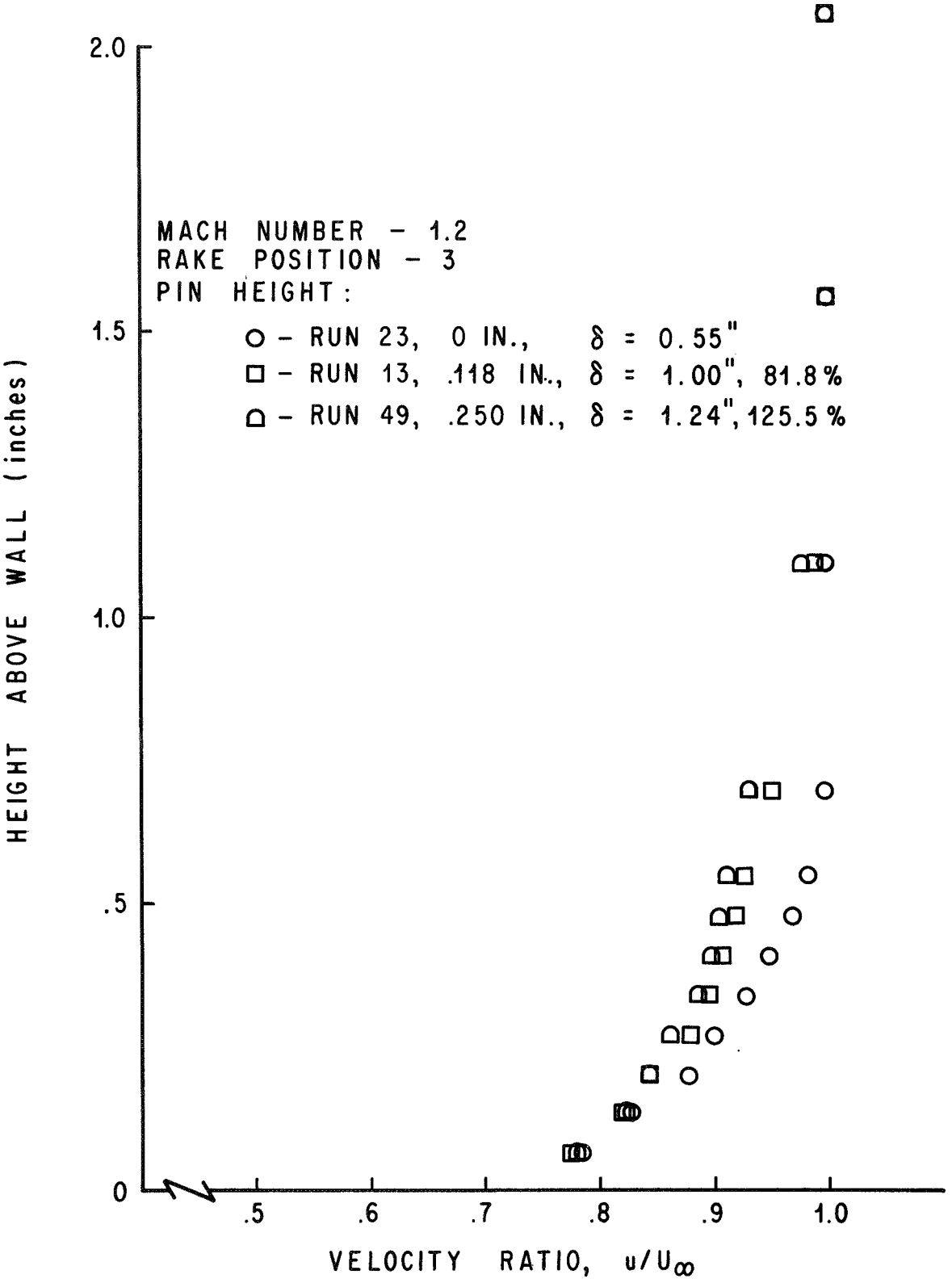
MACH NUMBER - 1.2
RAKE POSITION - 3
PIN HEIGHT:
○ - RUN 23, 0 IN., δ = 0.55"
□ - RUN 13, .118 IN., δ = 1.00", 81.8%
□ - RUN 49, .250 IN., δ = 1.24", 125.5%
HEIGHT ABOVE WALL (inches)
2.0
1.5
1.0
.5
0
.5
.6
.7
.8
.9
1.0
VELOCITY RATIO, u/U∞

FIGURE 5c

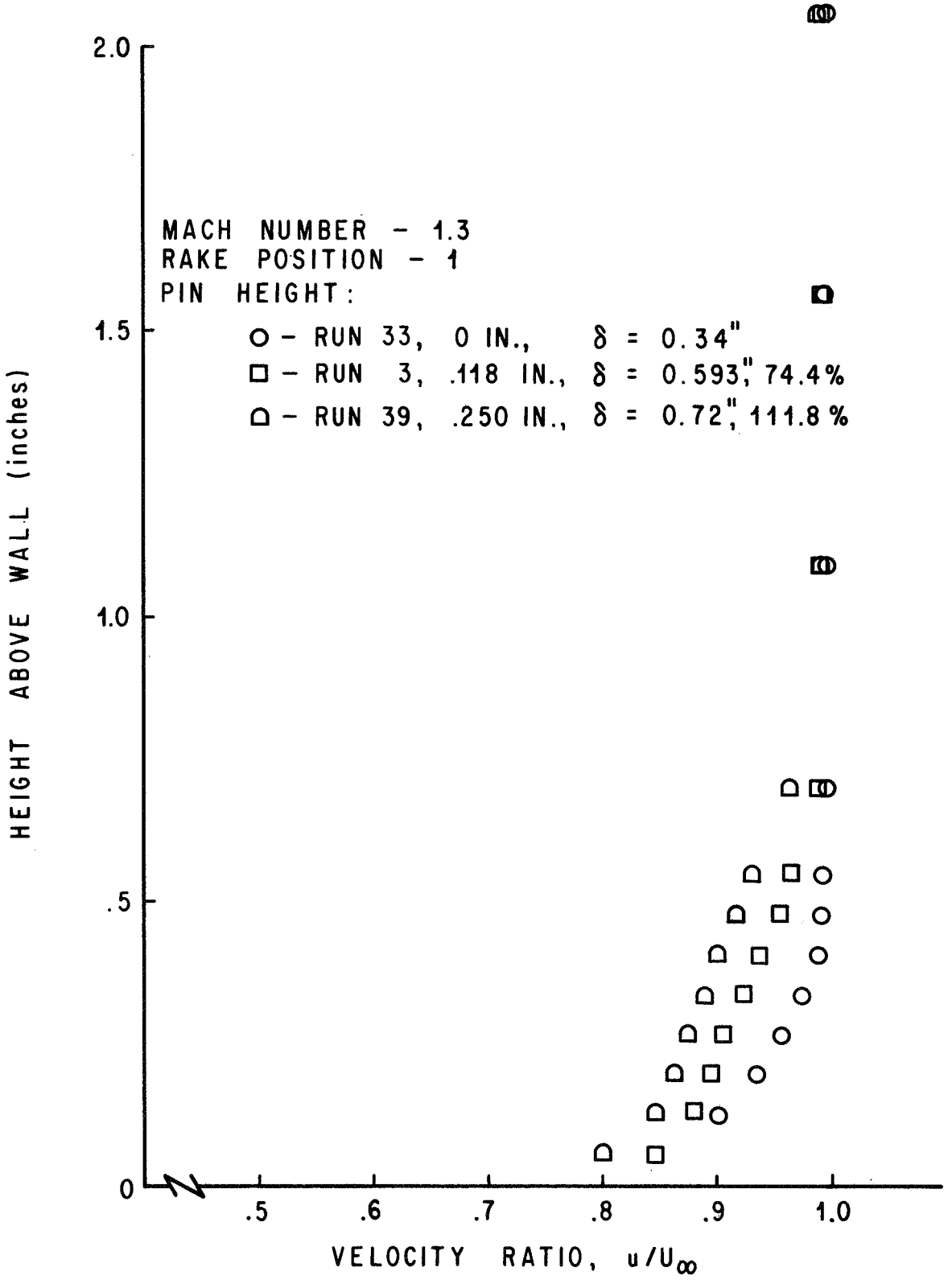
MACH NUMBER - 1.3
RAKE POSITION - 1
PIN HEIGHT:
O - RUN 33, 0 IN., δ = 0.34"
□ - RUN 3, .118 IN., δ = 0.593", 74.4%
Δ - RUN 39, .250 IN., δ = 0.72", 111.8%
HEIGHT ABOVE WALL (inches)
2.0
1.5
1.0
.5
0
.5
.6
.7
.8
.9
1.0
VELOCITY RATIO, u/U∞

FIGURE 5d

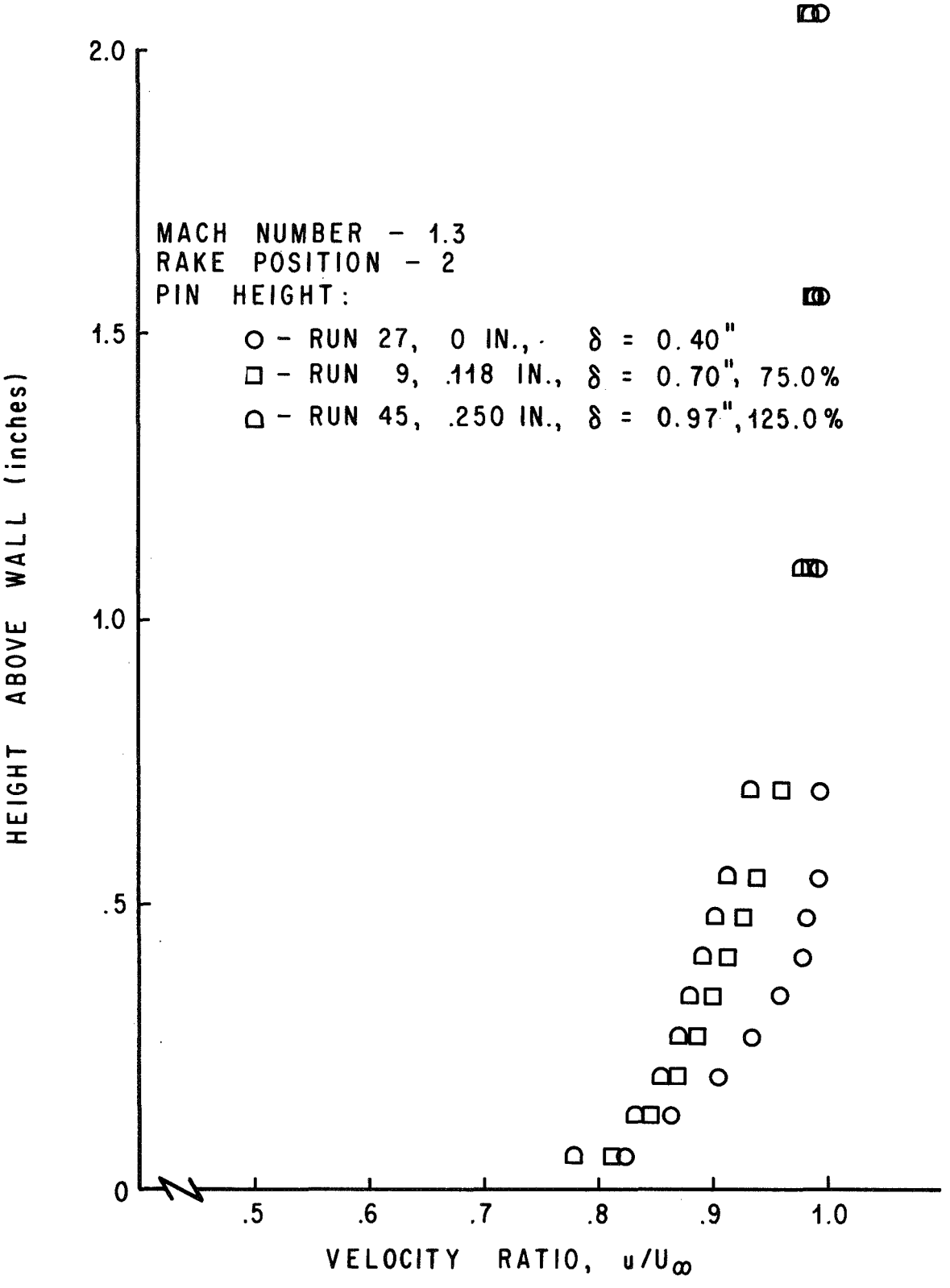
MACH NUMBER - 1.3
RAKE POSITION - 2
PIN HEIGHT:
○ - RUN 27, 0 IN., δ = 0.40"
□ - RUN 9, .118 IN., δ = 0.70", 75.0%
⌂ - RUN 45, .250 IN., δ = 0.97", 125.0%
HEIGHT ABOVE WALL (inches)
2.0
1.5
1.0
.5
0
.5
.6
.7
.8
.9
1.0
VELOCITY RATIO, u/U∞

FIGURE 5e

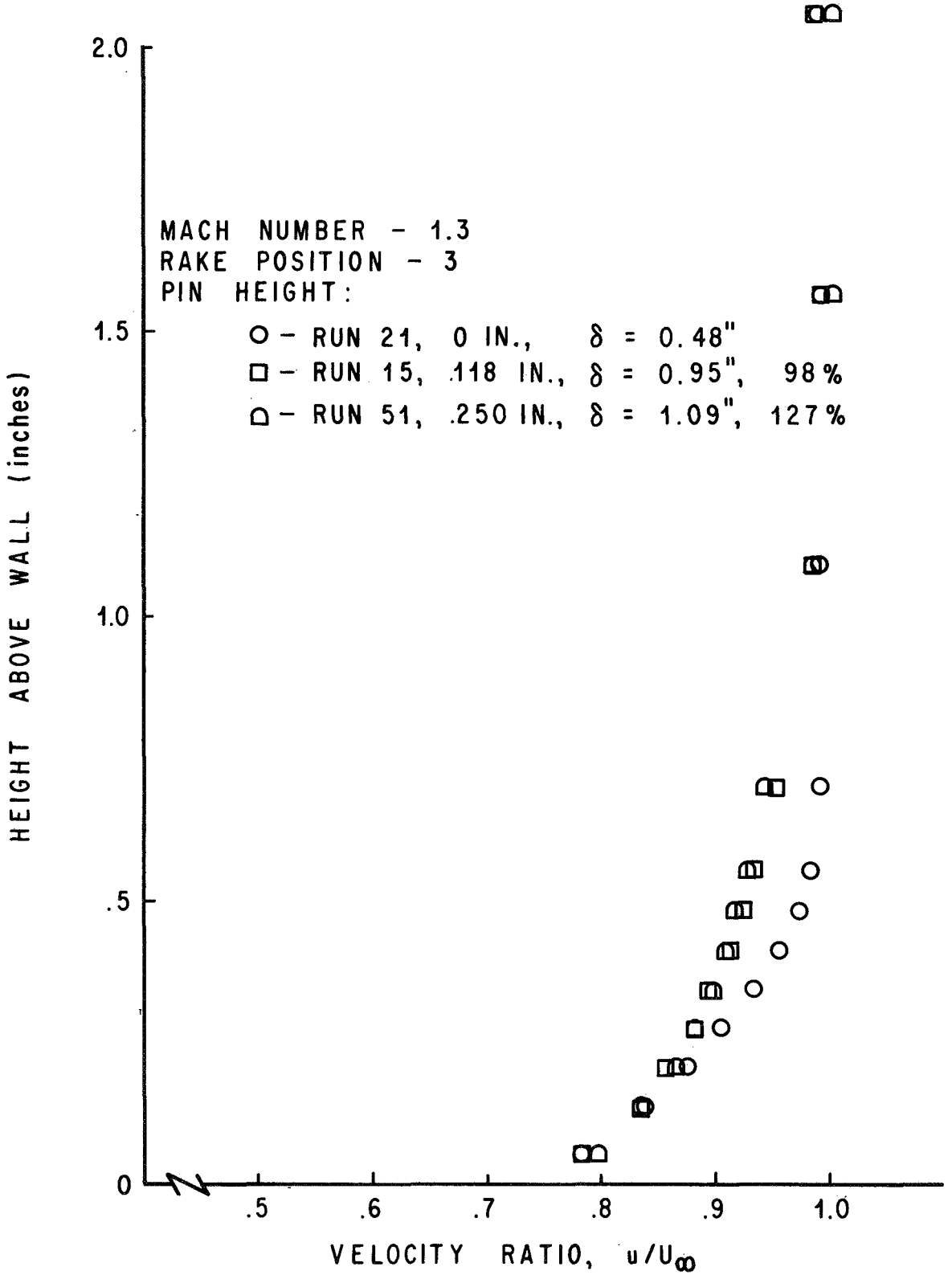
MACH NUMBER - 1.3
RAKE POSITION - 3
PIN HEIGHT:
O - RUN 21, 0 IN., δ = 0.48"
□ - RUN 15, .118 IN., δ = 0.95", 98%
△ - RUN 51, .250 IN., δ = 1.09", 127%
HEIGHT ABOVE WALL (inches)
2.0
1.5
1.0
.5
0
.5
.6
.7
.8
.9
1.0
VELOCITY RATIO, u/U∞

FIGURE 5f

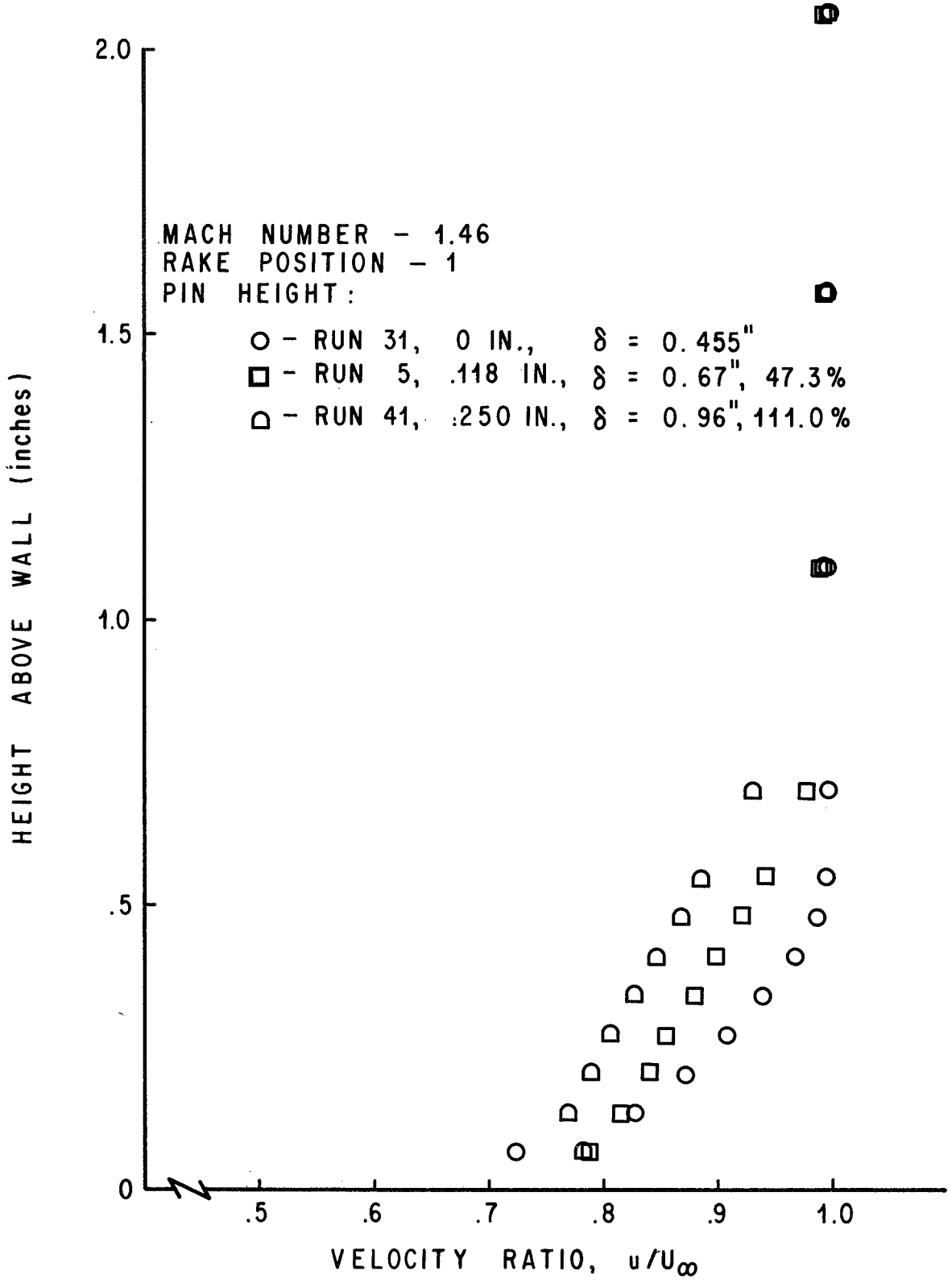
MACH NUMBER – 1.46
RAKE POSITION – 1
PIN HEIGHT:
○ – RUN 31, 0 IN., δ = 0.455"
□ – RUN 5, .118 IN., δ = 0.67", 47.3%
⌂ – RUN 41, .250 IN., δ = 0.96", 111.0%
HEIGHT ABOVE WALL (inches)
2.0
1.5
1.0
.5
0
.5
.6
.7
.8
.9
1.0
VELOCITY RATIO, u/U∞

FIGURE 5g

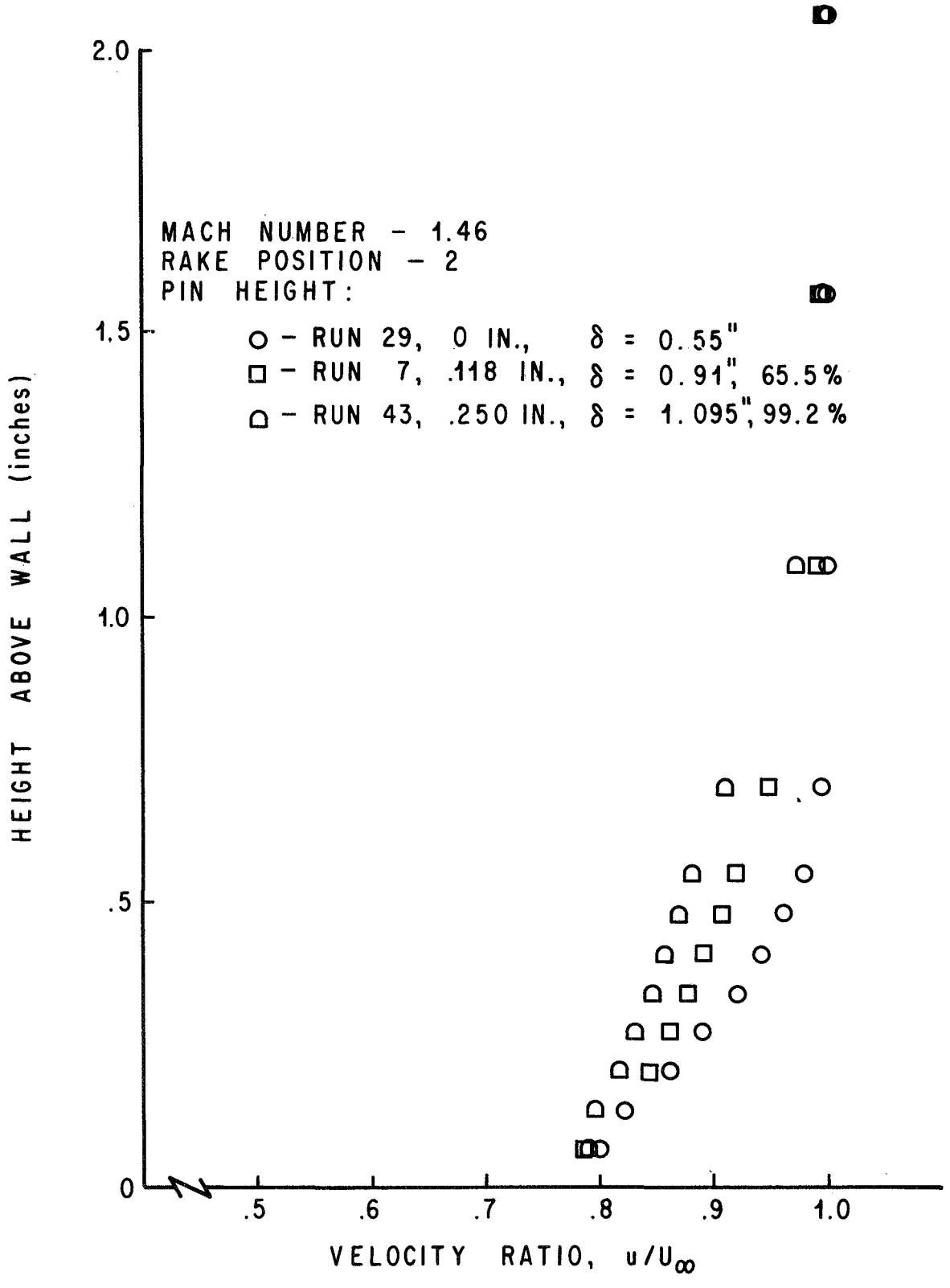
MACH NUMBER - 1.46
RAKE POSITION - 2
PIN HEIGHT:
○ - RUN 29, 0 IN., δ = 0.55"
□ - RUN 7, .118 IN., δ = 0.91", 65.5%
⌂ - RUN 43, .250 IN., δ = 1.095", 99.2%
HEIGHT ABOVE WALL (inches)
2.0
1.5
1.0
.5
0
.5
.6
.7
.8
.9
1.0
VELOCITY RATIO, u/U∞

FIGURE 5h

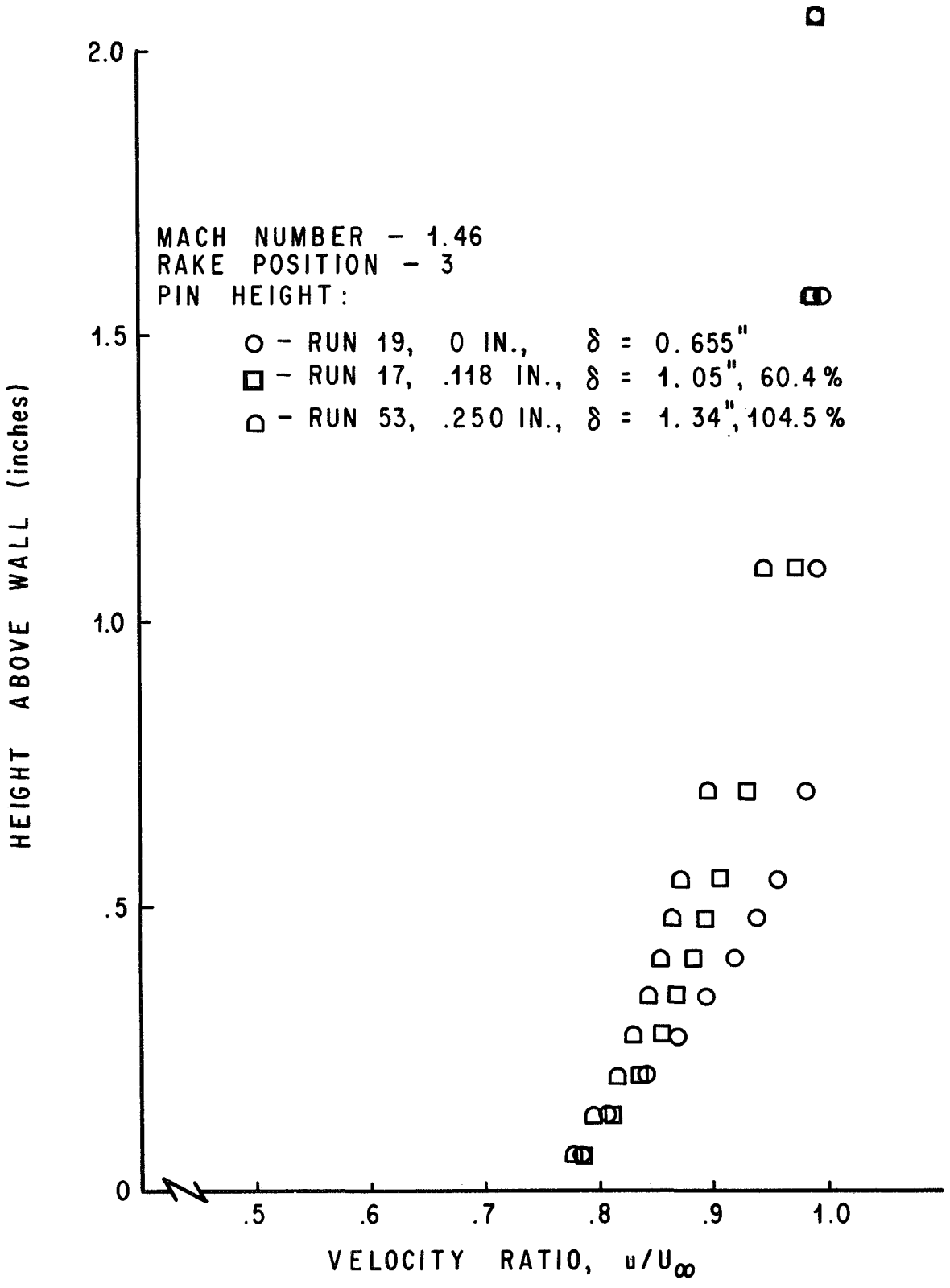
MACH NUMBER – 1.46
RAKE POSITION – 3
PIN HEIGHT:
○ – RUN 19, 0 IN., δ = 0.655"
□ – RUN 17, .118 IN., δ = 1.05", 60.4%
⌂ – RUN 53, .250 IN., δ = 1.34", 104.5%
HEIGHT ABOVE WALL (inches)
2.0
1.5
1.0
.5
0
.5
.6
.7
.8
.9
1.0
VELOCITY RATIO, u/U∞

FIGURE 5 i

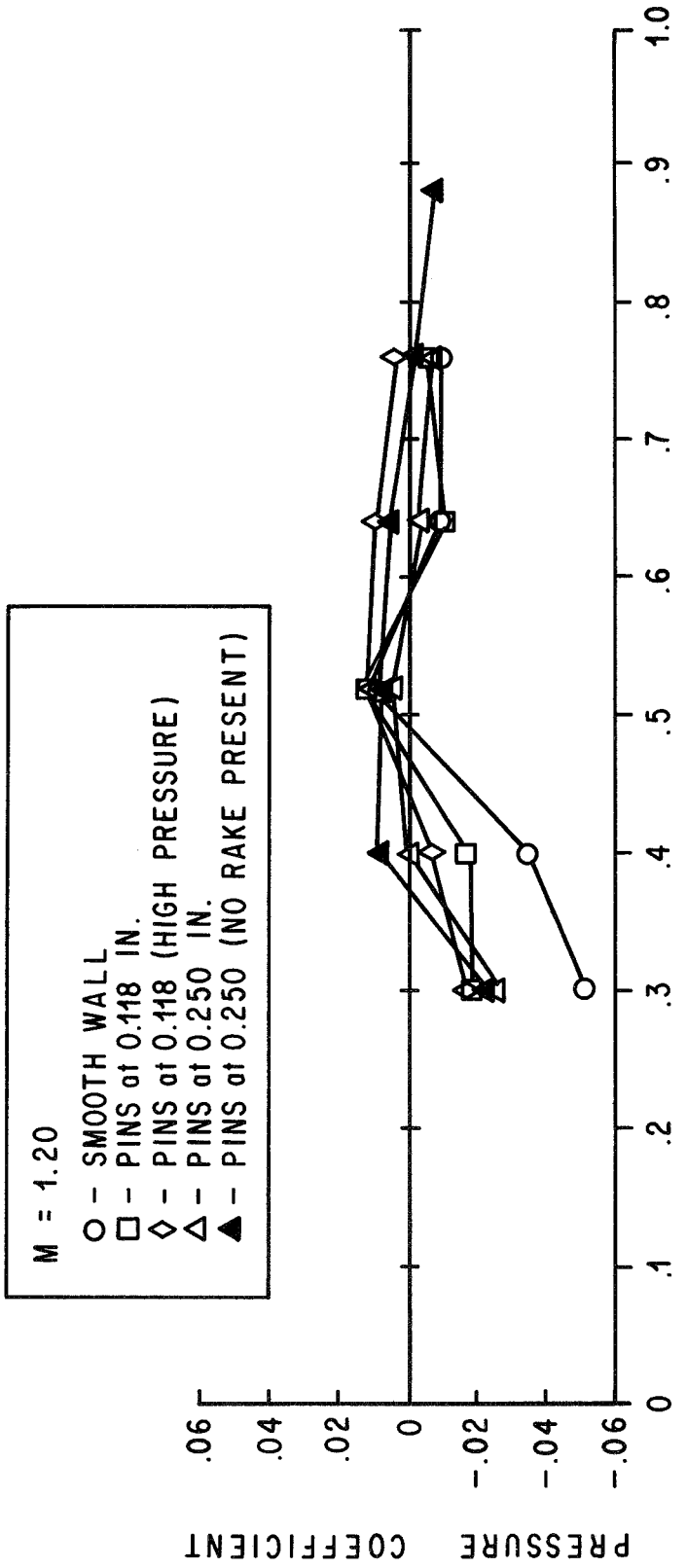


FIGURE 6a. PRESSURE COEFFICIENT VARIATION ALONE THE PLATE

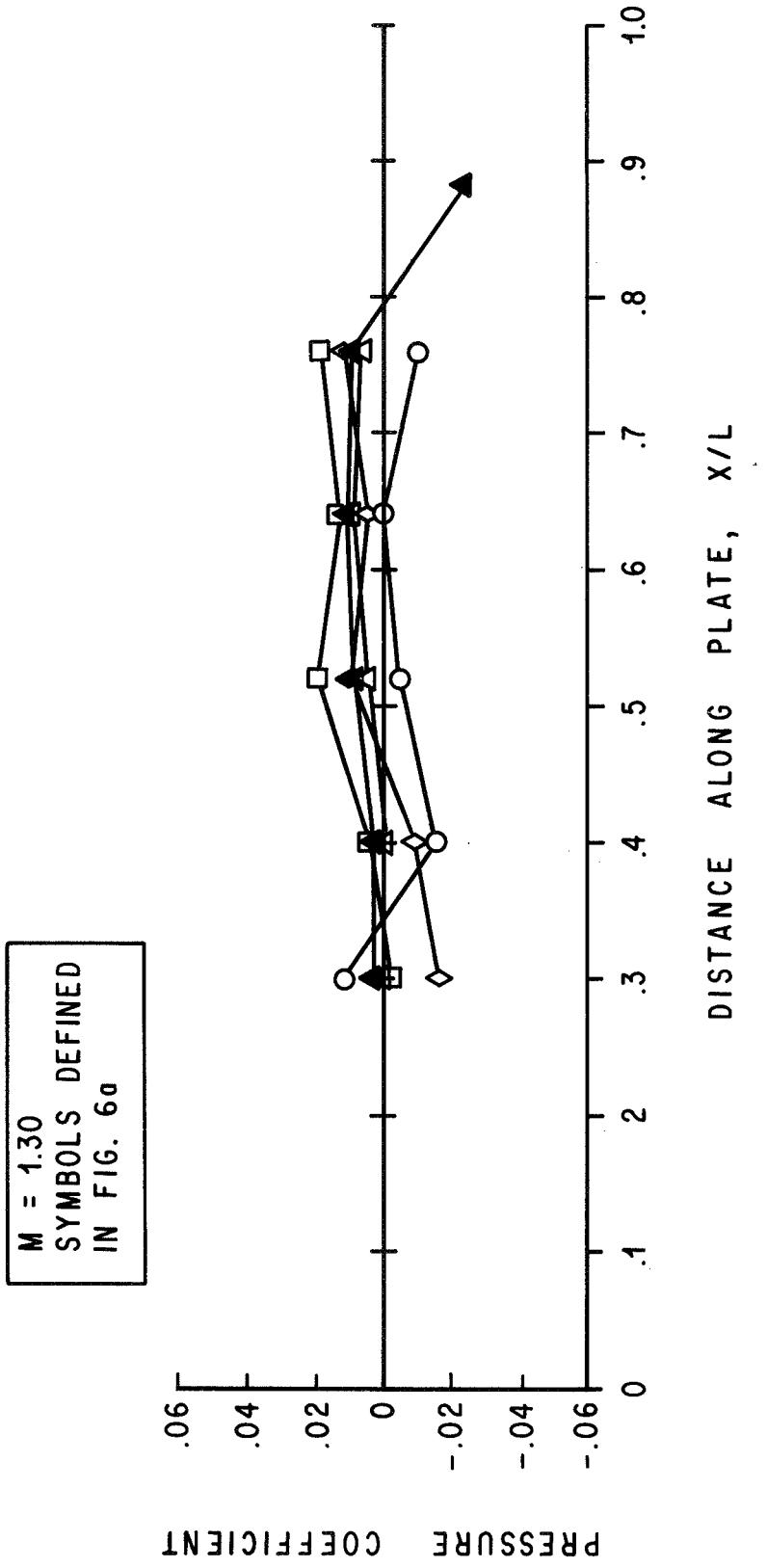
M = 1.30
SYMBOLS DEFINED
IN FIG. 6a
PRESSURE COEFFICIENT
.06
.04
.02
0
-.02
-.04
-.06
0
.1
.2
.3
.4
.5
.6
.7
.8
.9
1.0
DISTANCE ALONG PLATE, X/L

FIGURE 6b

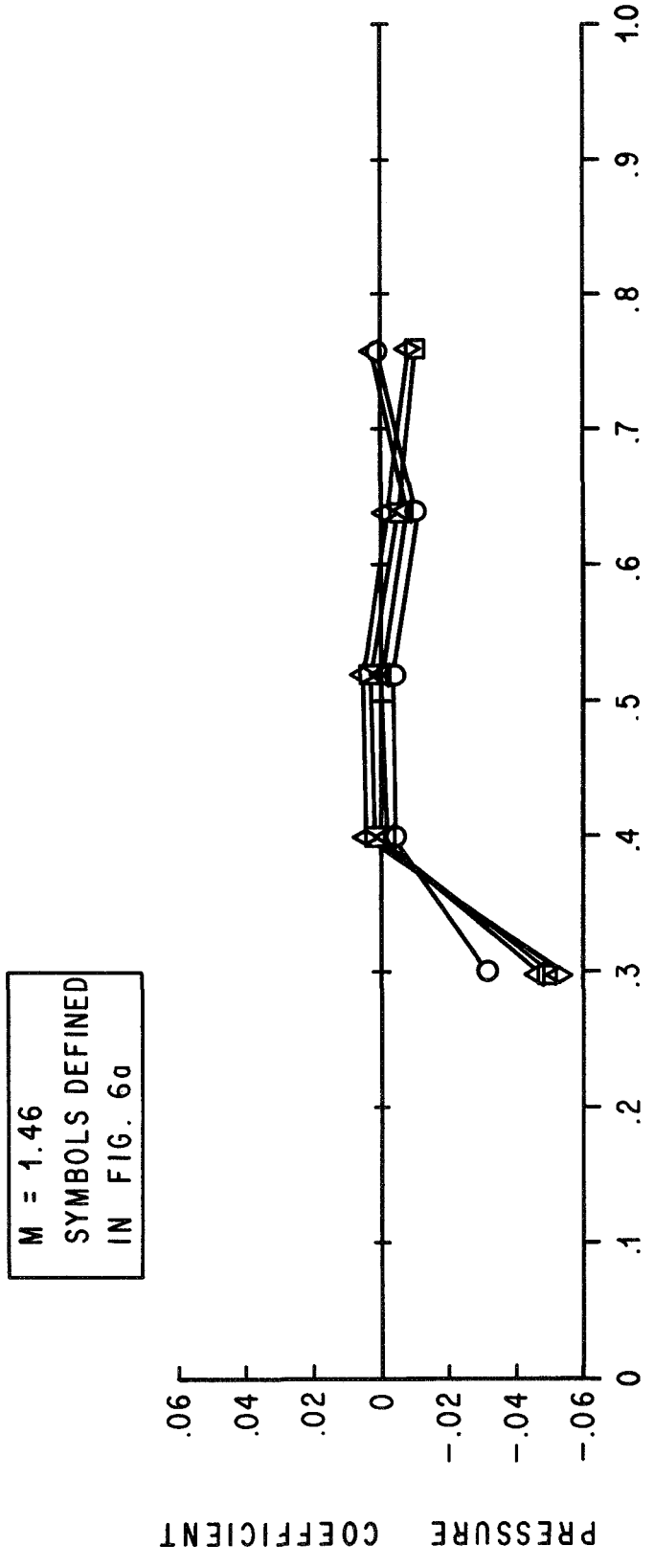
M = 1.46
SYMBOLS DEFINED
IN FIG. 6a
PRESSURE COEFFICIENT
.06
.04
.02
0
-.02
-.04
-.06
0
.1
.2
.3
.4
.5
.6
.7
.8
.9
1.0
DISTANCE ALONG PLATE, X/L

FIGURE 6c

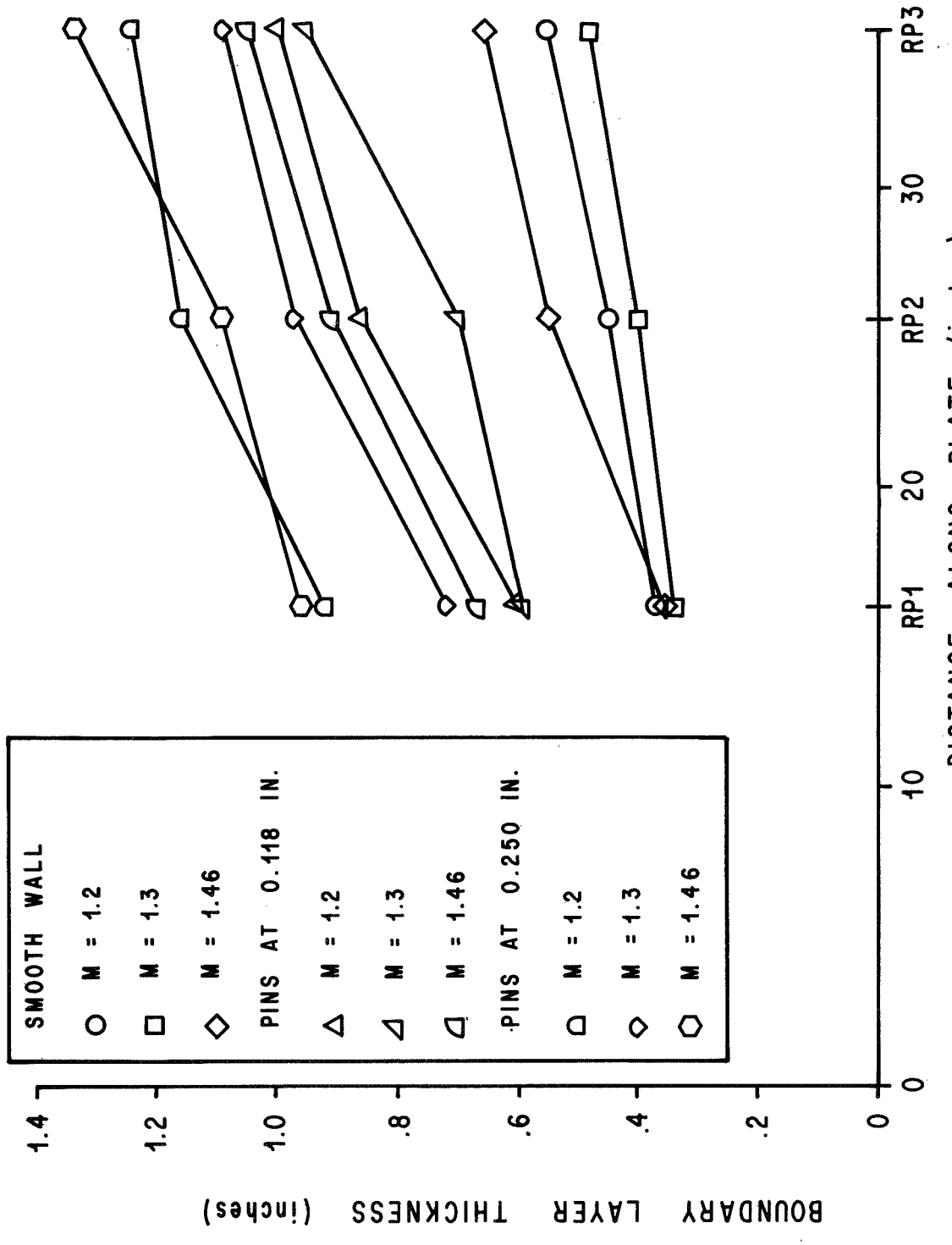


FIGURE 7. BOUNDARY LAYER GROWTH

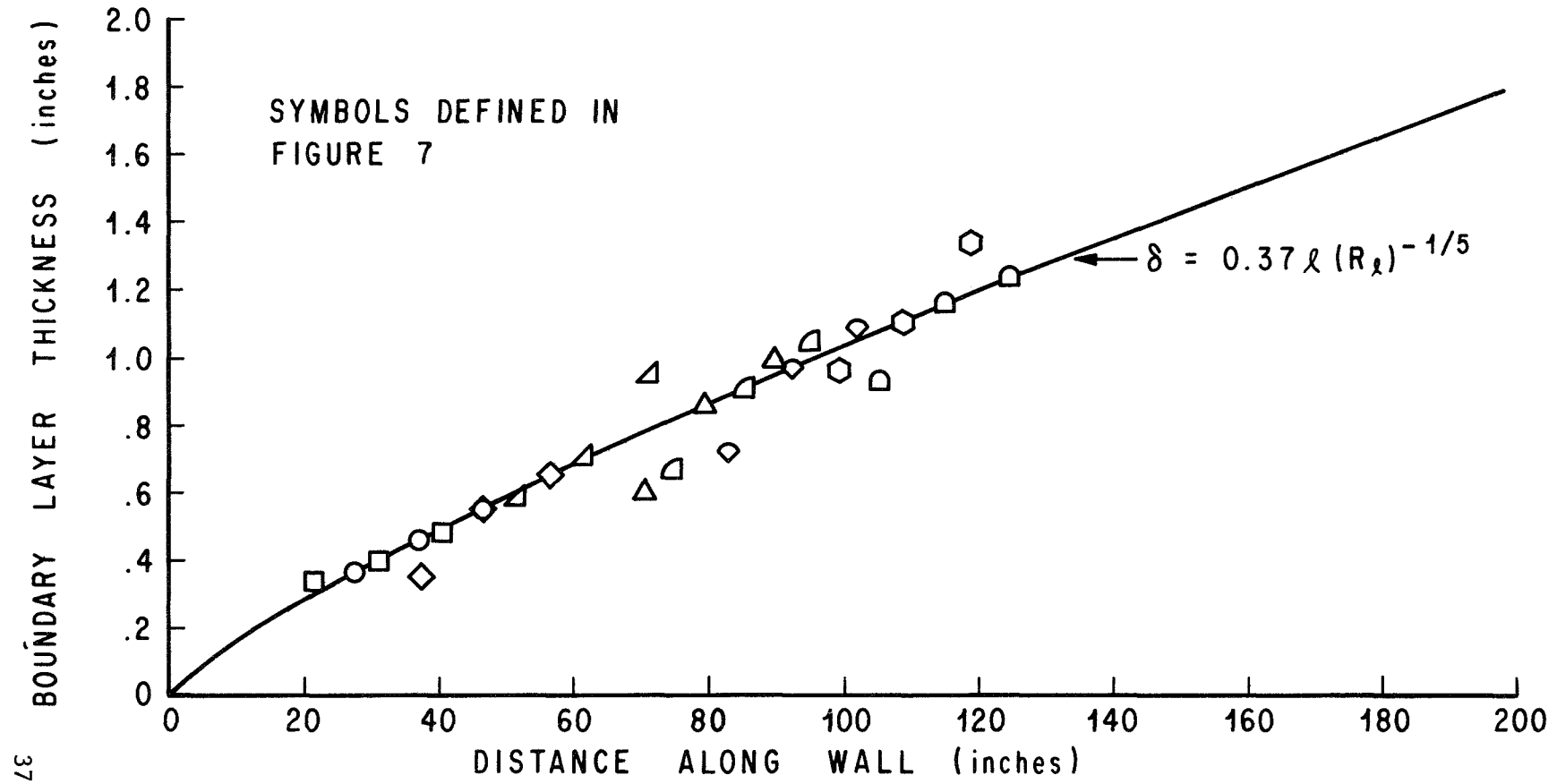


FIGURE 8. DATA COMPARED WITH TURBULENT BOUNDARY LAYER GROWTH

APPROVAL NASA TM X-53899

# RESULTS OF AN EXPERIMENTAL TURBULENT BOUNDARY LAYER CONTROL INVESTIGATION

by William W. Clever, II

The information in this report has been reviewed for security classification. Review of any information concerning Department of Defense or Atomic Energy Commission programs has been made by the MSFC Security Classification Officer. This report, in its entirety, has been determined to be unclassified.

This document has also been reviewed and approved for technical accuracy.

R. G. Beranek
Chief, Theory Section

T. G. Reed
Chief, Unsteady Gasdynamics Branch

W. K. Dahm
Chief, Aerophysics Division

E. D. Geissler
Director, Aero-Astrodynamics Laboratory

DISTRIBUTION

DIR
DEP-T
A&TS-PAT
A&TS-MS-H
A&TS-MS-IP
A&TS-MS-IL (8)
A&TS-TU (6)

S&E-AERO
Dr. Geissler
Mr. W. Vaughan
Dr. Lovingood
Mr. Lindberg
Mr. Baker
Mr. Dahm
Mr. Holderer
Mr. Felix
Mr. Cope (10)
Mr. Wilson
Mr. Linsley
Mr. Reed
Mr. Wilhold
Mr. Dunn
Mr. Andrews
Mr. Clever (30)

EXTERNAL

McDonnell Douglas Corporation
McDonnell Aircraft Co.
Bldg. 32; Level 2; Dept. 236
Lambert-St. Louis Municipal Airport
St. Louis, Missouri 63166
Attn: Dr. Zimmerman
Dr. Lemley
Mr. Kappus

Douglas Aircraft Co.
Group ABD1; Dept. 263
3000 Ocean Park Blvd.
Santa Monica, Calif.
Attn: Mr. Ailman

Ames Res. Center, NASA
Moffett Field, Calif. 94035
Experimental Investigations Br.
Attn: Mr. Fahey
Mr. Petroff

Tech. & Sci. Info. Facility (25)
Attn: NASA Rep. (S-AK/RKT)
Box 33
College Park, Md.

Aeronautical Systems Library
Bldg. 1408
NAS Whiting Field
Milton, Fla. 32570